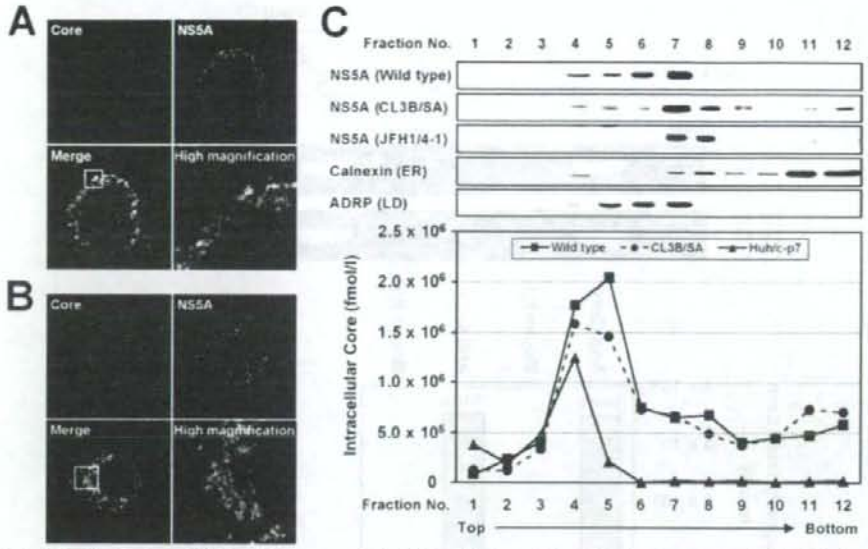

FIG. 7. Subcellular localization of NS5A and the core protein in HCV-replicating cells. Huh-7 cells were transfected with the in vitro transcript of the HCV genome, wild type (A) or CL3B/SA (B). Seventy-two hours after transfection, the cells were fixed with 4% paraformaldehyde, permeabilized with 0.3% Triton X-100, and double stained with antibodies against the core protein (green) and NS5A (red), followed by staining with an Alexa Fluor 488- or Alexa Fluor 555-conjugated antibody. High-magnification panels are enlarged images of white squares in the merge panels. (C) HCV (wild type or CL3B/SA)-replicating cells, JFH1/4-1 cells harboring a subgenomic replicon of JFH-1, or Huh/c-p7 cells stably expressing JFH-1 structural proteins were lysed by freeze-thawing, and the cell lysates were fractionated on 5 to 25% iodixanol gradients. The distributions of NS5A, calnexin (ER marker), and ADRP (LD marker) were determined by immunoblotting, and those of the core protein were examined by core protein-specific ELISA.

(50). However, the mechanism by which NS proteins participate in virus assembly or the role of the interaction between structural and NS proteins in virus life cycles has not been fully elucidated. Here, we have clearly demonstrated that HCV NS5A interacts with the core protein in coimmunoprecipitation experiments not only with coexpression of each epitope-tagged protein but also with cells expressing the viral genome; and by using immunofluorescence and subcellular fractionation analysis, we have confirmed that mutations in CL3B abolish colocalization of NS5A and the core protein, presumably around LDs. In addition, the intracellular infectivity assay and IP-RT-PCR strongly suggest that impairment of the NS5A-core protein interaction results in disruption of virus production at an early stage of virion assembly. On the basis of the present results and findings in accompanying articles, one may infer the following events: newly synthesized HCV RNAs bound to NS5A are released from the replication complex-containing membrane compartment and can be captured by the core protein via interaction with domain III of NS5A at the surface of LDs or LD-associated membranes. Consequently, the viral RNAs are encapsidated, and virion assembly proceeds in the local environment. Recruitment of newly synthesized viral RNAs to the core protein could be important for efficient nucleocapsid formation in cells, where concentrations of the viral genome and the structural proteins are typically low, and may contribute to the selection of the viral genome to be packaged. Interaction between NS5A and the core protein has been previously reported, and the NS5A region containing an interferon sensitivity determining region and the PKR-binding sequence (aa 2212 to 2330) has been mapped to that required for binding with core protein by yeast two-hybrid and in vitro pull-down assays (13). However, involvement of domain III in the NS5A-core protein interaction was not analyzed in detail, and a role for the NS5A-core protein interaction in the HCV life cycle was not examined in that study.

A growing body of evidence points to phosphorylation of NS5A as being important in controlling HCV RNA replication. Although the degree and the requirement for its hyperphosphorylation diverge between different HCV isolates, mutations that are associated with increased replicative fitness of HCV replicons frequently lead to a reduced level of NS5A hyperphosphorylation (1, 5, 36). Inhibitors of serine/threonine protein kinases that block NS5A hyperphosphorylation facilitate replication of a non-culture-adapted replicon (3, 36). One model that has been proposed suggests that NS5A hyperphosphorylation negatively regulates HCV RNA replication by disrupting the interaction between NS5A and the vesicle-associated membrane protein-associated protein subtype A, a cellular factor considered necessary for efficient RNA replication (5). However, the regulatory role of the basal phosphorylation of NS5A in the viral life cycle is poorly understood. It has been reported that the C-terminal region of NS5A (aa 2350 to 2419)

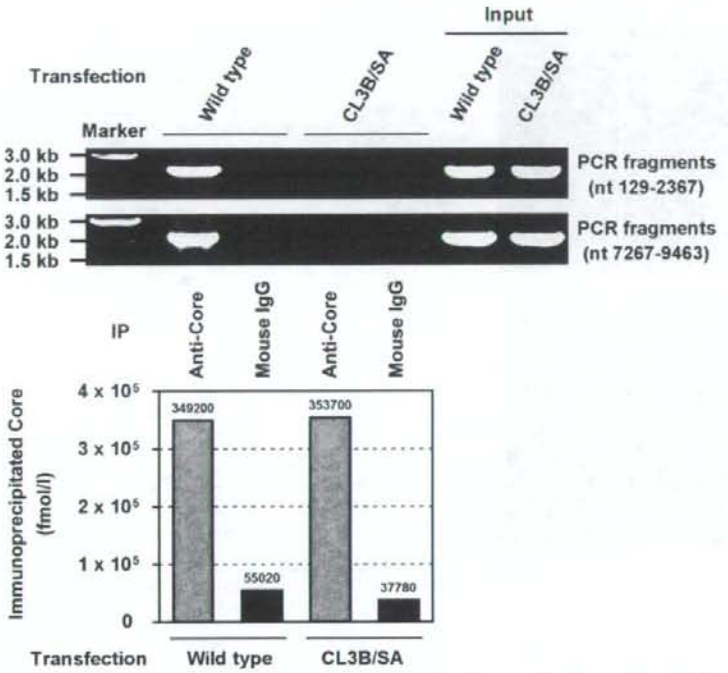

FIG. 8. IP-RT-PCR of HCV-replicating cells performed to examine the association between the core protein and the HCV genome RNA. Huh-7 cells were transfected with the in vitro transcript of the HCV genome (wild type or CL3B/SA) and lysed in 500 μl of hypotonic buffer at 72 h posttransfection. After IP with an anti-core protein antibody or mouse IgG, immunoprecipitates were eluted in 100 μl of elution buffer. RNAs in immunocomplexes were isolated by acid guanidinium thiocyanate-phenol-chloroform extraction. PCR was carried out as described in Materials and Methods with primer sets amplifying the fragments of nt 129 to 2367 and nt 7267 to 9463 of the JFH-1 genome. One-tenth (10 μl) of each eluted immunoprecipitate was used for assays of the core protein amounts to ensure IP efficiency (lower panel). RNA extracted from a small aliquot of each cell lysate used in IP-RT-PCR is shown as the input.

is involved in basal phosphorylation (23). There are highly conserved serine residues in this region, and alanine substitutions or in-frame deletion of the serine residues has been shown to impair basal phosphorylation but not to affect RNA replication in the genotype 1b isolate (1). Consistently, a metabolic ^{32}P labeling experiment in the present study demonstrated that NS5A mutants of the JFH-1 isolate in the region impair the basal phosphorylation. Nevertheless, Tellinghuisen et al. noted that the serine at aa 2433 of JFH-1 is involved in generating hyperphosphorylated NS5A, as shown by Western blotting (50). The basis for this difference is uncertain. To date, there is no clear evidence to determine which serine residues located in domain III are phosphoacceptor sites or whether these residues influence NS5A phosphorylation in an indirect fashion. Future study to map phosphoacceptor sites in the NS5A domain III by biochemical approaches is needed.

We found that two of the three serine residues at CL3B are responsible for regulating the interaction of NS5A with the core protein as well as for infectious virus production. To further evaluate the effect of constitutive serine phosphorylation at the cluster, we replaced the serine residues with glutamic acid, which mimics the presence of phosphoserines. The S2428/2430E mutant led to restoration of the interaction of NS5A with the core protein and virus production up to levels similar to the wild type. Somewhat unexpectedly, the triple glutamic acid substitution (CL3B/SE) exhibited only a slight restoration effect or none at all. It is considered that the degree of negative charge on the glutamic acid residue is not completely equivalent to that of phosphoserine. It is likely that the range of acidity at the local environment of the NS5A domain III that will allow interaction with the core protein is rather narrow. Induction of a conformational change in NS5A by the incorporation of phosphate may also be important for its interaction with the core protein. Tellinghuisen et al. reported that a single serine-to-alanine substitution at aa 2433 blocks the production of infectious virus and that casein kinase II likely phosphorylates the residue (50). Although this seems inconsistent with our results, these investigators also showed that deletions producing a lack of all three serine residues in the cluster inhibited virus production more severely than a single mutation. We observed that a single substitution of S2428A, S2430A, or S2433A resulted in a moderate decrease

in the virus released from the transfected cells; however, more evident perturbation was obtained from double or triple substitutions (Fig. 5A and B). Tellinghuisen et al. determined the HCV production at 48 h after RNA transfection and found a marked inhibition by the single substitution S2433A. In our study, as indicated in Fig. 5A, the reduction caused by the S2433A mutant was approximately 90% at 48 h after transfection; however, the virus production from the mutant reached a similar level to that of the wild type at 96 h posttransfection.

Several previous studies have found that apolipoproteins B (apoB) and E (apoE), microsomal triglyceride transfer protein, and HCV p7 protein are key factors for production of the infectious HCV particles (4, 11, 16, 22, 47). Assembly and maturation of the viral particles appear to depend on the formation of very-low-density lipoprotein, a large particle containing apoB, apoE, and large amounts of neutral lipids in hepatic cells. p7 protein is primarily involved in a late step of virus particle production, and the findings support the idea that p7 acts as viroporin, which has the capacity to compromise cell membrane integrity and thus favors the release of viral progeny. How the early step in virion production regulated by the NS5A-core protein interaction links with the later step(s) involved in the very-low-density lipoprotein assembly or p7 function remains an interesting question to be addressed.

In summary, we demonstrated that the C-terminal serine cluster of NS5A (aa 2428, 2430, and 2433), which is involved in generating the basal phosphorylated form, is a determinant of NS5A interaction with the core protein and the subcellular localization of NS5A. Mutation of this cluster blocks the NS5A-core protein interaction, resulting in perturbation of association between the core protein and HCV RNA. It is thus tempting to consider that NS5A plays a key role in transporting the viral genome RNA synthesized by the replication complex to the surface of LDs or LD-associated membranes, where the core protein localizes, leading to facilitation of nucleocapsid formation. Structural analysis of the NS5A domain III-core protein complex should provide greater insight into the mode of interaction between these viral proteins. Identification of residues at the interface that are involved in important interactions will be of significant value in designing novel structure-based inhibitors to block the early step of HCV particle formation.

ACKNOWLEDGMENTS

We are grateful to Francis V. Chisari (The Scripps Research Institute) for providing Huh-7 cells. We thank M. Matsuda, S. Yoshizaki, T. Shimoji, M. Kaga, and M. Sasaki for technical assistance and T. Mizoguchi for secretarial work.

This work was supported by Grants-in-Aid from the Ministry of Health, Labor and Welfare; by the Program for Promotion of Fundamental Studies in Health Sciences of the Organization for Drug ADR Relief, R&D Promotion and Product Review of Japan (grant ID:01-3); by the Japan Society for the Promotion of Science; and by Research on Health Sciences focusing on Drug Innovation from the Japan Health Sciences Foundation, Japan. T.M. is the recipient of a Research Resident Fellowship from the Foundation for Promotion of Cancer Research in Japan.

REFERENCES

1. **Appel, N., T. Pietschmann, and R. Bartenschlager.** 2005. Mutational analysis of hepatitis C virus nonstructural protein 5A: potential role of differential phosphorylation in RNA replication and identification of a genetically flexible domain. J. Virol. **79:**3187–3194.
2. **Appel, N., M. Zayas, S. Miller, J. Krijnse-Locker, T. Schaller, P. Friebe, S. Kallis, U. Engel, and R. Bartenschlager.** 2008. Essential role of domain III of nonstructural protein 5A for hepatitis C virus infectious particle assembly. PLoS Pathog. **4:**e1000035.
3. **Bürckstümmer, T., M. Kriegs, J. Lupberger, E. K. Pauli, S. Schmittel, and E. Hildt.** 2006. Raf-1 kinase associates with hepatitis C virus NS5A and regulates viral replication. FEBS Lett. **580:**575–580.
4. **Chang, K. S., J. Jiang, Z. Cai, and G. Luo.** 2007. Human apolipoprotein E is required for infectivity and production of hepatitis C virus in cell culture. J. Virol. **81:**13783–13793.
5. **Evans, M. J., C. M. Rice, and S. P. Goff.** 2004. Phosphorylation of hepatitis C virus nonstructural protein 5A modulates its protein interactions and viral RNA replication. Proc. Natl. Acad. Sci. USA **101:**13038–13043.
6. **Gale, M., Jr., C. M. Blakely, B. Kwieciszewski, S. L. Tan, M. Dossett, N. M. Tang, M. J. Korth, S. J. Polyak, D. R. Gretch, and M. G. Katze.** 1998. Control of PKR protein kinase by hepatitis C virus nonstructural 5A protein: molecular mechanisms of kinase regulation. Mol. Cell. Biol. **18:**5208–5218.
7. **Gale, M., Jr., and M. G. Katze.** 1998. Molecular mechanisms of interferon resistance mediated by viral-directed inhibition of PKR, the interferon-induced protein kinase. Pharmacol. Ther. **78:**29–46.
8. **Gale, M., Jr., B. Kwieciszewski, M. Dossett, H. Nakao, and M. G. Katze.** 1999. Antiapoptotic and oncogenic potentials of hepatitis C virus are linked to interferon resistance by viral repression of the PKR protein kinase. J. Virol. **73:**6506–6516.
9. **Gale, M. J., Jr., M. J. Korth, and M. G. Katze.** 1998. Repression of the PKR protein kinase by the hepatitis C virus NS5A protein: a potential mechanism of interferon resistance. Clin. Diagn. Virol. **10:**157–162.
10. **Gale, M. J., Jr., M. J. Korth, N. M. Tang, S. L. Tan, D. A. Hopkins, T. E. Dever, S. J. Polyak, D. R. Gretch, and M. G. Katze.** 1997. Evidence that hepatitis C virus resistance to interferon is mediated through repression of the PKR protein kinase by the nonstructural 5A protein. Virology **230:**217–227.
11. **Gastaminza, P., G. Cheng, S. Wieland, J. Zhong, W. Liao, and F. V. Chisari.** 2008. Cellular determinants of hepatitis C virus assembly, maturation, degradation, and secretion. J. Virol. **82:**2120–2129.
12. **Gastaminza, P., S. B. Kapadia, and F. V. Chisari.** 2006. Differential biophysical properties of infectious intracellular and secreted hepatitis C virus particles. J. Virol. **80:**11074–11081.
13. **Goh, P. Y., Y. J. Tan, S. P. Lim, S. G. Lim, Y. H. Tan, and W. J. Hong.** 2001. The hepatitis C virus core protein interacts with NS5A and activates its caspase-mediated proteolytic cleavage. Virology **290:**224–236.
14. **Hicke, L., B. Zanolari, and H. Riezman.** 1998. Cytoplasmic tail phosphorylation of the alpha-factor receptor is required for its ubiquitination and internalization. J. Cell Biol. **141:**349–358.
15. **Hoofnagle, J. H.** 2002. Course and outcome of hepatitis C. Hepatology **36:**S21–S29.
16. **Huang, H., F. Sun, D. M. Owen, W. Li, Y. Chen, M. Gale, Jr., and J. Ye.** 2007. Hepatitis C virus production by human hepatocytes dependent on assembly and secretion of very low-density lipoproteins. Proc. Natl. Acad. Sci. USA **104:**5848–5853.
17. **Huang, L., J. Hwang, S. D. Sharma, M. R. Hargittai, Y. Chen, J. J. Arnold, K. D. Raney, and C. E. Cameron.** 2005. Hepatitis C virus nonstructural protein 5A (NS5A) is an RNA-binding protein. J. Biol. Chem. **280:**36417–36428.
18. **Ishii, K., K. Murakami, S. S. Hmwe, B. Zhang, J. Li, M. Shirakura, K. Morikawa, R. Suzuki, T. Miyamura, T. Wakita, and T. Suzuki.** 2008. Transencapsidation of hepatitis C virus subgenomic replicon RNA with viral structure proteins. Biochem. Biophys. Res. Commun. **371:**446–450.
19. **Ishii, K., Y. Ueda, K. Matsuo, Y. Matsuura, T. Kitamura, K. Kato, Y. Izumi, K. Someya, T. Ohsu, M. Honda, and T. Miyamura.** 2002. Structural analysis of vaccinia virus DIs strain: application as a new replication-deficient viral vector. Virology **302:**433–444.
20. **Jesch, S. A., A. J. Mehta, M. Velliste, R. F. Murphy, and A. D. Linstedt.** 2001. Mitotic Golgi is in a dynamic equilibrium between clustered and free vesicles independent of the ER. Traffic **2:**873–884.
21. **Johnson, R. F., S. E. McCarthy, P. J. Godlewski, and R. N. Harty.** 2006. Ebola virus VP35-VP40 interaction is sufficient for packaging 3E–5E minigenome RNA into virus-like particles. J. Virol. **80:**5135–5144.
22. **Jones, C. T., C. L. Murray, D. K. Eastman, J. Tassello, and C. M. Rice.** 2007. Hepatitis C virus p7 and NS2 proteins are essential for production of infectious virus. J. Virol. **81:**8374–8383.
23. **Kaneko, T., Y. Tanji, S. Satoh, M. Hijikata, S. Asabe, K. Kimura, and K. Shimotohno.** 1994. Production of two phosphoproteins from the NS5A region of the hepatitis C viral genome. Biochem. Biophys. Res. Commun. **205:**320–326.
24. **Kato, T., T. Date, M. Miyamoto, M. Sugiyama, Y. Tanaka, E. Orito, T. Ohno, K. Sugihara, I. Hasegawa, K. Fujiwara, K. Ito, A. Ozasa, M. Mizokami, and T. Wakita.** 2005. Detection of anti-hepatitis C virus effects of interferon and ribavirin by a sensitive replicon system. J. Clin. Microbiol. **43:**5679–5684.
25. **Kümmerer, B. M., and C. M. Rice.** 2002. Mutations in the yellow fever virus nonstructural protein NS2A selectively block production of infectious particles. J. Virol. **76:**4773–4784.

26. **Leung, J. Y., G. P. Pijlman, N. Kondratieva, J. Hyde, J. M. Mackenzie, and A. A. Khromykh.** 2008. Role of nonstructural protein NS2A in flavivirus assembly. J. Virol. **82:**4731–4741.
27. **Liang, T. J., B. Rehermann, L. B. Seeff, and J. H. Hoofnagle.** 2000. Pathogenesis, natural history, treatment, and prevention of hepatitis C. Ann. Intern. Med. **132:**296–305.
28. **Lindenbach, B. D., M. J. Evans, A. J. Syder, B. Wolk, T. L. Tellinghuisen, C. C. Liu, T. Maruyama, R. O. Hynes, D. R. Burton, J. A. McKeating, and C. M. Rice.** 2005. Complete replication of hepatitis C virus in cell culture. Science **309:**623–626.
29. **Liu, W. J., H. B. Chen, and A. A. Khromykh.** 2003. Molecular and functional analyses of Kunjin virus infectious cDNA clones demonstrate the essential roles for NS2A in virus assembly and for a nonconservative residue in NS3 in RNA replication. J. Virol. **77:**7804–7813.
30. **Liu, W. J., P. L. Sedlak, N. Kondratieva, and A. A. Khromykh.** 2002. Complementation analysis of the flavivirus Kunjin NS3 and NS5 proteins defines the minimal regions essential for formation of a replication complex and shows a requirement of NS3 in *cis* for virus assembly. J. Virol. **76:**10766–10775.
31. **Manns, M. P., H. Wedemeyer, and M. Cornberg.** 2006. Treating viral hepatitis C: efficacy, side effects, and complications. Gut **55:**1350–1359.
32. **Miyamoto, M., T. Kato, T. Date, M. Mizokami, and T. Wakita.** 2006. Comparison between subgenomic replicons of hepatitis C virus genotypes 2a (JFH-1) and 1b (Con1 NK5.1). Intervirology **49:**37–43.
33. **Miyanari, Y., K. Atsuzawa, N. Usuda, K. Watashi, T. Hishiki, M. Zayas, R. Bartenschlager, T. Wakita, M. Hijikata, and K. Shimotohno.** 2007. The lipid droplet is an important organelle for hepatitis C virus production. Nat. Cell Biol. **9:**1089–1097.
34. **Moradpour, D., M. J. Evans, R. Gosert, Z. Yuan, H. E. Blum, S. P. Goff, B. D. Lindenbach, and C. M. Rice.** 2004. Insertion of green fluorescent protein into nonstructural protein 5A allows direct visualization of functional hepatitis C virus replication complexes. J. Virol. **78:**7400–7409.

34a. **Murakami, K., T. Kimura, M. Osaki, K. Ishii, T. Miyamura, T. Suzuki, T. Wakita, and I. Shoji.** 2008. Virological characterization of the hepatitis C virus JFH-1 strain in lymphocytic cell lines. J. Gen. Virol. **89:**1587–1592.

35. **National Institutes of Health.** 2002. NIH consensus statement on management of hepatitis C: NIH Consens. State. Sci. Statements **19:**1–46.
36. **Neddermann, P., M. Quintavalle, C. Di Pietro, A. Clementi, M. Cerretani, S. Altamura, L. Bartholomew, and R. De Francesco.** 2004. Reduction of hepatitis C virus NS5A hyperphosphorylation by selective inhibition of cellular kinases activates viral RNA replication in cell culture. J. Virol. **78:**13306–13314.
37. **Niwa, H., K. Yamamura, and J. Miyazaki.** 1991. Efficient selection for high-expression transfectants with a novel eukaryotic vector. Gene **108:**193–199.
38. **Pawlotsky, J. M.** 1999. Hepatitis C virus (HCV) NS5A protein: role in HCV replication and resistance to interferon-alpha. J. Viral Hepat. **6**(Suppl. 1): 47–48.
39. **Pawlotsky, J. M., G. Germanidis, A. U. Neumann, M. Pellerin, P. O. Frainais, and D. Dhumeaux.** 1998. Interferon resistance of hepatitis C virus genotype 1b: relationship to nonstructural 5A gene quasispecies mutations. J. Virol. **72:**2795–2805.
40. **Poynard, T., M. F. Yuen, V. Ratziu, and C. L. Lai.** 2003. Viral hepatitis C. Lancet **362:**2095–2100.
41. **Schaller, T., N. Appel, G. Koutsoudakis, S. Kallis, V. Lohmann, T. Pietschmann, and R. Bartenschlager.** 2007. Analysis of hepatitis C virus superinfection exclusion by using novel fluorochrome gene-tagged viral genomes. J. Virol. **81:**4591–4603.
42. **Seeff, L. B., and J. H. Hoofnagle.** 2003. Appendix: The National Institutes of Health Consensus Development Conference: management of hepatitis C 2002. Clin. Liver Dis. **7:**261–287.
43. **Seeff, L. B., and J. H. Hoofnagle.** 2002. National Institutes of Health Consensus Development Conference: management of hepatitis C: 2002. Hepatology **36:**S1–S2.
44. **Shavinskaya, A., S. Boulant, F. Penin, J. McLauchlan, and R. Bartenschlager.** 2007. The lipid droplet binding domain of hepatitis C virus core protein is a major determinant for efficient virus assembly. J. Biol. Chem. **282:**37158–37169.
45. **Shi, S. T., S. J. Polyak, H. Tu, D. R. Taylor, D. R. Gretch, and M. M. Lai.** 2002. Hepatitis C virus NS5A colocalizes with the core protein on lipid droplets and interacts with apolipoproteins. Virology **292:**198–210.
46. **Shirakura, M., K. Murakami, T. Ichimura, R. Suzuki, T. Shimoji, K. Fukuda, K. Abe, S. Sato, M. Fukasawa, Y. Yamakawa, M. Nishijima, K. Moriishi, Y. Matsuura, T. Wakita, T. Suzuki, P. M. Howley, T. Miyamura, and I. Shoji.** 2007. E6AP ubiquitin ligase mediates ubiquitylation and degradation of hepatitis C virus core protein. J. Virol. **81:**1174–1185.
47. **Steinmann, E., F. Penin, S. Kallis, A. H. Patel, R. Bartenschlager, and T. Pietschmann.** 2007. Hepatitis C virus p7 protein is crucial for assembly and release of infectious virions. PLoS Pathog. **3:**e103.
48. **Tan, S. L., and M. G. Katze.** 2001. How hepatitis C virus counteracts the interferon response: the jury is still out on NS5A. Virology **284:**1–12.
49. **Tanji, Y., T. Kaneko, S. Satoh, and K. Shimotohno.** 1995. Phosphorylation of hepatitis C virus-encoded nonstructural protein NS5A. J. Virol. **69:**3980–3986.
50. **Tellinghuisen, T. L., K. L. Foss, and J. Treadaway.** 2008. Regulation of hepatitis C virion production via phosphorylation of the NS5A protein. PLoS Pathog. **4:**e1000032.
51. **Tellinghuisen, T. L., K. L. Foss, J. C. Treadaway, and C. M. Rice.** 2008. Identification of residues required for RNA replication in domains II and III of the hepatitis C virus NS5A protein. J. Virol. **82:**1073–1083.
52. **Tellinghuisen, T. L., J. Marcotrigiano, A. E. Gorbalenya, and C. M. Rice.** 2004. The NS5A protein of hepatitis C virus is a zinc metalloprotein. J. Biol. Chem. **279:**48576–48587.
53. **Tellinghuisen, T. L., J. Marcotrigiano, and C. M. Rice.** 2005. Structure of the zinc-binding domain of an essential component of the hepatitis C virus replicase. Nature **435:**374–379.
54. **van den Hoff, M. J., A. F. Moorman, and W. H. Lamers.** 1992. Electroporation in "intracellular" buffer increases cell survival. Nucleic Acids Res. **20:**2902.
55. **van Regenmortel, M. H. V., C. M. Fauquet, D. H. L. Bishop, E. B. Carstens, M. K. Estes, S. M. Lemon, J. Maniloff, M. A. Mayo, D. J. McGeoch, C. R. Pringle, and R. B. Wickner (ed.).** 2000. Virus taxonomy: classification and nomenclature of viruses. Seventh report of the International Committee on Taxonomy of Viruses. Academic Press, San Diego, CA.
56. **Wakita, T., T. Pietschmann, T. Kato, T. Date, M. Miyamoto, Z. Zhao, K. Murthy, A. Habermann, H. G. Krausslich, M. Mizokami, R. Bartenschlager, and T. J. Liang.** 2005. Production of infectious hepatitis C virus in tissue culture from a cloned viral genome. Nat. Med. **11:**791–796.
57. **Watashi, K., M. Hijikata, A. Tagawa, T. Doi, H. Marusawa, and K. Shimotohno.** 2003. Modulation of retinoid signaling by a cytoplasmic viral protein via sequestration of Sp110b, a potent transcriptional corepressor of retinoic acid receptor, from the nucleus. Mol. Cell. Biol. **23:**7498–7509.
58. **Zhong, J., P. Gastaminza, G. Cheng, S. Kapadia, T. Kato, D. R. Burton, S. F. Wieland, S. L. Uprichard, T. Wakita, and F. V. Chisari.** 2005. Robust hepatitis C virus infection in vitro. Proc. Natl. Acad. Sci. USA **102:**9294–9299.

JOURNAL OF VIROLOGY, June 2008, p. 5715–5724 Vol. 82, No. 12
0022-538X/08/$08.00+0 doi:10.1128/JVI.02530-07

Critical Role of Virion-Associated Cholesterol and Sphingolipid in Hepatitis C Virus Infection▽

Hideki Aizaki,[1] Kenichi Morikawa,[1] Masayoshi Fukasawa,[2] Hiromichi Hara,[1] Yasushi Inoue,[1] Hideki Tani,[3] Kyoko Saito,[2] Masahiro Nishijima,[2] Kentaro Hanada,[2] Yoshiharu Matsuura,[3] Michael M. C. Lai,[4] Tatsuo Miyamura,[1] Takaji Wakita,[1] and Tetsuro Suzuki[1]*

Department of Virology II[1] and Department of Biochemistry and Cell Biology,[2] National Institute of Infectious Diseases, Tokyo 162-8640, and Department of Molecular Virology, Research Institute for Microbial Diseases, Osaka University, Osaka 565-0871,[3] Japan, and Department of Molecular Microbiology and Immunology, University of Southern California, Los Angeles, California 90033-1054[4]

Received 27 November 2007/Accepted 17 March 2008

In this study, we establish that cholesterol and sphingolipid associated with hepatitis C virus (HCV) particles are important for virion maturation and infectivity. In a recently developed culture system enabling study of the complete life cycle of HCV, mature virions were enriched with cholesterol as assessed by the molar ratio of cholesterol to phospholipid in virion and cell membranes. Depletion of cholesterol from the virus or hydrolysis of virion-associated sphingomyelin almost completely abolished HCV infectivity. Supplementation of cholesterol-depleted virus with exogenous cholesterol enhanced infectivity to a level equivalent to that of the untreated control. Cholesterol-depleted or sphingomyelin-hydrolyzed virus had markedly defective internalization, but no influence on cell attachment was observed. Significant portions of HCV structural proteins partitioned into cellular detergent-resistant, lipid-raft-like membranes. Combined with the observation that inhibitors of the sphingolipid biosynthetic pathway block virion production, but not RNA accumulation, in a JFH-1 isolate, our findings suggest that alteration of the lipid composition of HCV particles might be a useful approach in the design of anti-HCV therapy.

Hepatitis C virus (HCV) is recognized as a major cause of chronic liver disease, including chronic hepatitis, hepatic steatosis, cirrhosis, and hepatocellular carcinoma. It presently affects approximately 200 million people worldwide (26). HCV is an enveloped positive-strand RNA virus belonging to the *Hepacivirus* genus of the family *Flaviviridae*. Its genome of ~9.6 kb encodes a polyprotein precursor of ~3,000 residues, and the structural proteins (core, E1, and E2) reside in its N-terminal region.

Little is known about the assembly of HCV and its virion structure, because efficient production of authentic HCV particles has only recently been achieved. Nucleocapsid assembly generally involves oligomerization of the capsid protein and encapsidation of genomic RNA. This process is thought to occur upon interaction of the core protein with viral RNA, and this core-RNA interaction may induce a change from RNA replication to packaging. As with related viruses, the mature HCV virion likely consists of a nucleocapsid and an outer envelope composed of a lipid membrane and envelope proteins. Expression of the structural proteins in mammalian cells has been observed to generate virus-like particles with ultrastructural properties similar to those of HCV virions (5, 29). Packaging of these HCV-like particles into intracellular vesicles as a result of budding from the endoplasmic reticulum (ER) has also been observed (8, 34). However, HCV structural proteins are observed both in the ER and in the Golgi apparatus (45). Moreover, complex N-linked glycans have been detected on the surfaces of HCV particles isolated from patient sera, suggesting that the glycans transit through the Golgi apparatus (44). Interactions between the core and E1/E2 proteins are thought to determine viral morphology and are mediated through a cytoplasmic loop present in the polytopic form of E1 (35). Recently, we and others have identified a unique HCV genotype 2a isolate, JFH-1, that is able to replicate and produce high levels of infectious virus in culture (HCVcc) (54, 56), enabling us to investigate new aspects of the HCV life cycle.

In this study, we examine the importance of cholesterol and sphingolipid in association with the HCV membrane in virion maturation and virus infectivity. Mature HCV particles are rich in cholesterol. Cholesterol depletion or hydrolysis of sphingolipid from HCV particles results in a loss of infectivity. We further demonstrate a requirement for virion-associated cholesterol and sphingolipid for viral entry.

MATERIALS AND METHODS

Cell culture. The human hepatoma cell line Huh-7, which is permissive to HCV infection, was obtained from Francis V. Chisari (The Scripps Research Institute). Human embryonic kidney 293T cells were cultured in Dulbecco's modified Eagle medium (DMEM)–10% fetal bovine serum. Huh-7 cell lines, which carry subgenomic replicon RNA of either the JFH-1 (20) or the N (11, 17) strain, were cultured as previously described (21, 46).

Reagents. The primary antibodies used in this study were mouse monoclonal antibodies against vesicular stomatitis virus glycoprotein (VSV-G) (Sigma, St. Louis, MO), HCV E1 (54) and E2 (Biodesign International, Saco, ME), caveolin-2 (New England Biolabs, Beverly, MA), and CD81 (BD Pharmingen, Franklin Lakes, NJ), as well as rabbit polyclonal antibodies against calnexin (Stressgen, Ann Arbor, MI) and HCV core (48). ISP-1/myriocin, cholesterol, and

* Corresponding author. Mailing address: Department of Virology II, National Institute of Infectious Diseases, 1-23-1 Toyama, Shinjuku-ku, Tokyo 162-8640, Japan. Phone: 81 3 5285 1111. Fax: 81 3 5285 1161. E-mail: tesuzuki@nih.go.jp.

▽ Published ahead of print on 26 March 2008.

heparinase I were purchased from Sigma, and recombinant *Bacillus cereus* sphingomyelinase (SMase) was obtained from Higeta Shoyu (Tokyo, Japan). (*1R,3R*)-*N*-(3-Hydroxy-1-hydroxymethyl-3-phenylpropyl) dodecanamide (HPA-12), which was synthesized as described elsewhere (24), was a gift from Shu Kobayashi (University of Tokyo).

Plasmids. pCAE1 and pCAE2 contain HCV cDNAs spanning the E1 region (amino acids 192 to 383) with a FLAG tag at the N terminus and the E2 region (amino acids 384 to 809) with a Myc tag at the N terminus of strain NIIJ1 (1), respectively, under the control of the CAG promoter (38). pCAV340V and pCAV711V consist of the ectodomains of E1 and E2, respectively, with the N-terminal signal sequences, transmembrane domains, and cytoplasmic domains derived from VSV-G, as described elsewhere (50) (see Fig. 4D).

Virus production. Plasmid pJFH1, containing full-length cDNA of the JFH-1 isolate, was used to generate HCVcc as described elsewhere (23, 33, 34, 54). pJ6/JFH1 was obtained from JFH1 by replacement of the 5′ untranslated region to the p7 region (EcoRI-BclI) of J6. In vitro-transcribed RNA from linearized pJFH1 or pJ6/JFH1 was delivered to Huh-7 cells by electroporation. Culture supernatants were collected at 72 h posttransfection, clarified by low-speed centrifugation, passed through a 0.45-mm-pore-size filter, and concentrated using an Amicon Ultra-15 unit (Millipore, Bedford, MA) or by ultracentrifugation (23). Infectious titers, HCV RNA copies, and core protein concentrations of the viral stocks were $\sim 5 \times 10^5$ focus-forming units per ml, $\sim 1 \times 10^7$ copies/ml, and $\sim 1 \times 10^4$ fmol/liter, respectively. HCVcc was isolated by a combination of ultrafiltration, ion-exchange chromatography, heparin affinity chromatography, and sucrose density ultracentrifugation (33; K. Morikawa and T. Wakita, unpublished data). Pseudotyped VSV containing E1 and E2 proteins of the HCV genotype 1a isolate H77c (HCVpv) was generated as previously described (51). Briefly, 293T cells transiently expressing E1 and E2 proteins (strain H77) were infected with VSVdelG-GFP/G, in which the G envelope gene was replaced with green fluorescent protein (GFP) and pseudotyped with VSV-G.

Determination of cholesterol and phospholipid contents of HCVcc and infected cells. Cellular and viral lipids were extracted from isolated HCVcc and from uninfected and infected Huh-7 cells. Cholesterol content was determined using the cholesterol oxidase method as previously described (14). Total phospholipid content was determined using the method of Rouser et al. (42).

Cholesterol depletion and replacement. To remove cholesterol from the HCV envelope, stock samples of HCVcc were treated with *methyl*-β-cyclodextrin (B-CD) in DMEM (Sigma) supplemented with 10% fetal bovine serum (Sigma) and nonessential amino acids (Invitrogen, Carlsbad, CA) for 1 h at 37°C, followed by centrifugation at 100,000 × *g* for 3 h to form a pellet, which was resuspended in 0.5 ml of the medium. In order to replenish cholesterol, the medium of HCVcc treated with 5 mg/ml B-CD was replaced with DMEM containing various concentrations of exogenous cholesterol (Sigma) and incubated for 1 h, followed by centrifugation to form a pellet. In order to perform HCVcc infection assays, Huh-7 cells were infected with HCVcc, with or without the treatment described above, for 1 h at 37°C and then washed as described above. Viral core protein levels in the cells and in the supernatant were quantified 72 h later using an HCV core enzyme-linked immunosorbent assay (Ortho-Clinical Diagnostics, Tokyo, Japan).

SMase treatment. HCVcc was treated with SMase at various concentrations in DMEM for 1 h at 37°C and was then centrifuged at 100,000 × *g* for 3 h to form a pellet, which was resuspended in 0.5 ml of medium for the infection assays.

HCVcc binding and internalization assays. To monitor binding, cells grown in a 6-well plate were preincubated for 1 h at 4°C, after which B-CD- or SMase-treated HCVcc was bound to the cells for 1 h at 4°C. As a measure of virus internalization, following the virus binding procedure, the cells were warmed to 37°C and maintained for 2 h, after which they were treated with 0.25% trypsin for 10 min at 37°C. Huh7-25, a CD81-negative Huh-7 subclone (3), was used to ensure removal of surface-bound virus by trypsin treatment. For both the binding and internalization assays, the resulting cells, as described above, were washed with ice-cold phosphate-buffered saline, followed by lysis with TRIzol reagent (Invitrogen). Cell-associated virus was quantified by measuring the amount of HCV RNA in the cell lysate by the real-time reverse transcription-PCR method (2, 34). Cells were treated with heparinase as previously described (33).

HCV replication assay in HCVcc-infected or replicon cells. HCV subgenomic replicon cells or cells infected with HCVcc were treated with various concentrations of inhibitors for 72 h. Total RNA was isolated from replicon cells using TRIzol reagent (Invitrogen), followed by quantification of HCV RNA by real-time reverse transcription-PCR as previously described (2, 34). Levels of core protein in the culture supernatants of HCVcc-infected cells were tested as described above.

Detection of cholesterol content of HCVcc. For [^{3}H]cholesterol labeling of viruses, HCVcc-infected or uninfected cells were incubated with 50 mCi of [1α,2α-^{3}H]cholesterol in DMEM for 24 h. Culture supernatants of the cells were incubated in the presence or absence of B-CD at 5 mg/ml for 1 h at 37°C, followed by ultracentrifugation on a 60% sucrose cushion. The virus-containing fractions and corresponding fractions from an uninfected culture were lysed in the buffer containing 1% Triton X-100 (TX-100), and radioactivity was quantified by scintillation counting. Radioactivities (in counts per minute) of HCVcc samples were determined by subtracting the radioactivity of uninfected cells from that of HCVcc-infected cells.

TABLE 1. Cholesterol and phospholipid contents of HCVcc and cells

Cell type or virus	Content (nmol/mg of protein)[a]		Chol/PL ratio
	Chol	PL	
Cells			
Uninfected	105.9 ± 10.4	253.2 ± 10.6	0.42
JFH-1 infected	116.5 ± 10.0	292.0 ± 18.4	0.40
Virus			
JFH-1	43.6 ± 2.4	33.8 ± 1.8	1.29
J6/JFH-1[b]	28.7 ± 4.8	22.7 ± 2.9	1.26

[a] Data are averages of three independent measurements ± standard deviations. Chol, cholesterol; PL, phospholipids.
[b] J6/JFH1 virus was produced from the pJ6/N2X-JFH1 construct and has structural proteins from the J6CF strain.

Metabolic labeling analysis of sphingolipid content. After 2 h of incubation with [^{14}C]serine (0.5 mCi/ml) in Opti-MEM (Invitrogen), the cells were lysed with 0.1% sodium dodecyl sulfate, and total lipid was extracted with chloroform-methanol (1:2, vol/vol). The extracts were spotted onto silica gel 60 plates (Merck, Darmstadt, Germany) and chromatographed with methyl acetate–1-propanol–chloroform–methanol–0.25% KCl (25:25:25:10:9, vol/vol). Radioactive spots were quantitatively detected by BAS 2000 (Fuji Film, Japan).

Membrane flotation assay. The membrane flotation assay was performed as previously described (46).

RESULTS

Critical role of virion-associated cholesterol. A role of virion-associated cholesterol in infectivity has been demonstrated for several enveloped viruses (4). However, little is known about the role of lipids associated with the virions of flaviviruses, including HCV, and their contribution to the viral life cycle. To determine the lipid composition of mature HCV virions, we extracted total lipid from HCVcc (JFH-1 and chimeric J6/JFH-1) prepared from the culture supernatants of cells infected with HCV, as well as the total cellular membrane fractions of uninfected and infected Huh-7 cells. The cholesterol and phospholipid contents were quantified, because these are the two major lipid constituents of biological membranes. The cholesterol-to-phospholipid molar ratio, which is known as a parameter of membrane viscosity (47), was significantly higher in virus samples (1.29 and 1.26 for JFH-1 and J6/JFH-1, respectively) than in cell membrane samples (0.40 and 0.42 for JFH-1-infected and uninfected cells, respectively) (Table 1). The ratios in viral samples were similar to or greater than those in mammalian plasma membranes, where most cellular cholesterol is found. Minimal contamination of the viral samples with extracellular microvesicles likely occurred, since only a small amount of lipid was detected in a sample prepared from the culture medium of uninfected cells (data not shown). Thus, it is likely that HCV virions are enriched with cholesterol during assembly and maturation.

To investigate a potential role for the particular lipid composition of HCV particles, HCVcc was treated with

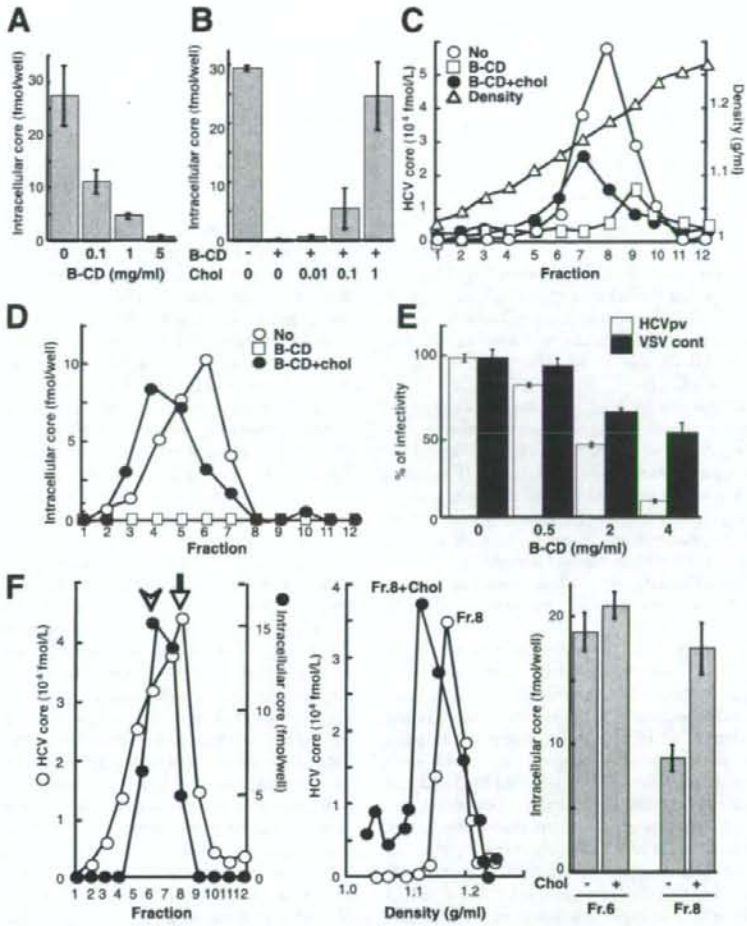

FIG. 1. Role of HCV-associated cholesterol in infection. (A) Effect of cholesterol depletion on HCV infectivity. HCVcc particles (~2 fmol of the core protein) were treated with B-CD at 0.1, 1, and 5 mg/ml for 1 h at 37°C. After removal of B-CD, Huh-7 cells were infected with the treated virus particles, after which the core protein content of infected cells at 72 h p.i. was determined as an indicator of infectivity, as previously established (24). (B) Effect of cholesterol replenishment on infectivity. After treatment with 5 mg/ml B-CD, virus was treated either with medium alone or with medium containing exogenous cholesterol for 1 h at 37°C. (C) Effect of cholesterol depletion and replenishment on density gradient profiles of the viral particles. The HCVcc treated with 5 mg/ml B-CD was replenished with exogenous cholesterol (1 mM) and then separated by 10-to-60% sucrose gradient ultracentrifugation. The core protein in each fraction was measured. The density of each fraction was determined by refractive index measurement. (D) Effects of cholesterol depletion and replenishment on viral infectivity. Each fraction (see panel C) was infected, and then the core proteins in the cells were measured at 72 h p.i. (E) Effect of cholesterol depletion on the infectivity of HCVpv (genotype 1a) (shaded bars) or the control, VSVdelG-GFP/G (solid bars). The viruses were preincubated with B-CD for 1 h at 37°C before infection. (F) (Left) The culture medium from HCVcc-producing cells was fractionated as described above. For each fraction, the amounts of core and intracellular core (infectivity) are plotted. Peaks of the core (arrow) and infectivity (arrowhead) are indicated. (Center) An aliquot of fraction 8 (peak of the core) was treated with 1 mM cholesterol for 1 h at 37°C. The resultant aliquot and an untreated aliquot of the fraction were subjected to sucrose gradient ultracentrifugation. The core in each fraction was plotted. (Right) The infectivities of fractions (Fr.) 6 and 8 (see the left panel) with or without cholesterol treatment were determined as shown above. Data are means from four independent experiments. Error bars, standard deviations.

increasing concentrations (0.1 to 5 mg/ml) of B-CD, which is known to extract cholesterol from membranes (40). The viral samples were then used to inoculate Huh-7 cells after removal of B-CD by ultracentrifugation. Infectivity was evaluated by quantifying the viral core protein in cells at 72 h postinfection (p.i.). Using an immunoassay that provides results indicative of HCV infectivity (25), we also confirmed a good correlation between the core level and

TABLE 2. Depletion of virion-associated cholesterol by B-CD

Treatment	Radioactivity (cpm) of HCVcc[a]		Avg (%[b])
	Expt 1	Expt 2	
None	5,327	5,573	5,450 (100)
B-CD (5 mg/ml)	3,643	1,646	2,644 (48.5)

[a] Determined by subtracting the radioactivity of uninfected cells from that of HCVcc-infected cells in two experiments.
[b] Percentage of the radioactivity of the untreated sample.

infectious titers (data not shown). As shown in Fig. 1A, core protein levels following B-CD treatment at 0.1, 1, or 5 mg/ml were reduced by 60, 83, or 98%, respectively, from the levels with the untreated virus. The cholesterol level of HCVcc treated with 5 mg/ml B-CD was found to be ~50% of that of untreated virions (Table 2).

To demonstrate that the reduced infection efficiency of B-CD-treated virus was caused by the reduced cholesterol content of the viral envelope, we attempted to reverse the inhibitory effect by adding exogenous cholesterol. Following treatment of HCVcc with 5 mg/ml B-CD, the drug was washed out, and increasing concentrations of cholesterol were added in an attempt to reconstitute the normal virion cholesterol content. The addition of 1 mM cholesterol completely reversed the virus infectivity (Fig. 1B). After cholesterol was replenished, the viral RNA was restored to a level similar to that in the untreated control.

To investigate the effect of cholesterol on the density of infectious HCV virions, B-CD-pretreated or untreated viral samples, as well as cholesterol-replenished treated viral samples, were subjected to sucrose density gradient centrifugation (Fig. 1C). The density of HCVcc core protein at its peak concentration in untreated virus samples was ~1.17 g/ml. When virion-associated cholesterol was removed by B-CD, the density of HCVcc core protein at its peak concentration was shifted to 1.20 g/ml. Addition of exogenous cholesterol to this cholesterol-depleted sample restored a lower-density fraction (1.15 g/ml). Figure 1D illustrates the infectivity of each gradient fraction. Untreated virus had maximum infectivity at ~1.13 g/ml (fraction 6), while, as expected, fractions from B-CD-treated viral samples exhibited minimal to no infectivity. Replenishment of depleted virus with cholesterol returned infectivity to untreated-control levels, and cholesterol-replenished virus had a buoyant density of ~1.07 g/ml (fraction 4), suggesting that HCV-associated cholesterol is crucial for viral infectivity and that the effect of a cholesterol-depleting drug is reversible. We further observed that B-CD treatment of a pseudotyped VSV containing the E1 and E2 proteins of the HCV genotype 1a isolate H77c (HCVpv) resulted in a progressive loss of infectivity, while B-CD had significantly less impact on the infectivity of the control virus VSVdelG-GFP/G (Fig. 1E).

The results described above raise the possibility that the infectivity of HCV virions with relatively low levels of incorporated cholesterol might be enhanced by supplementation with exogenous cholesterol. Density gradient fractions of culture supernatants collected from HCV-infected cells were analyzed with regard to the presence of core protein and infectivity (Fig. 1F, left). As indicated above, maximum infectivity was obtained with fraction 6 (1.13 g/ml). In contrast, a major fraction of core protein banded at a higher density (1.17 g/ml) in fraction 8. We hypothesized that fraction 8 contains lipids at lower levels than those in fraction 6. However, quantification of lipids, including cholesterol, in the fractions obtained failed, presumably due to a low sensitivity of detection. Thus, to extend our findings on the involvement of cholesterol, we added exogenous cholesterol to fraction 8, followed by ultrafiltration to remove unincorporated cholesterol. A subsequent density gradient profile demonstrated a shift in the core protein peak to 1.13 g/ml (Fig. 1F, center). A concomitant increase in the infectivity of the fraction, approaching that of untreated fraction 6, was observed (Fig. 1F, right). In contrast, supplementation of fraction 6 with exogenous cholesterol did not alter its infectivity (Fig. 1F, right) or change its density gradient (data not shown). These results suggest that exogenous cholesterol supplementation can reverse deficits in the infectivity of HCV virions due to low cholesterol content.

Sphingolipid dependence of HCV infectivity. In addition to cholesterol, sphingolipid is a major component of eukaryotic lipid membranes. We therefore investigated the functional significance of sphingomyelin (SM), the most abundant sphingolipid, with regard to HCV infectivity. HCVcc was treated for 1 h with increasing concentrations (0.1 to 10 U/ml) of bacterial SMase, which is known to hydrolyze membrane-bound SM to ceramide. Following ultracentrifugation to remove the SMase, Huh-7 cells were inoculated with the HCVcc. The amount of HCV core protein within the cells was quantified at 72 h p.i. Figure 2A shows 50 and 90% reductions in HCV infectivity after incubation of the virion with 0.1 and 1 U/ml SMase, respectively. We further observed that SMase treatment of HCVpv resulted in a progressive loss of infectivity, while SMase had no effect on the infectivity of the control virus (Fig. 2B). This demonstrates that sphingolipid, like cholesterol, plays an essential role in HCV infectivity.

Requirement for virion-associated cholesterol and sphingolipid during HCV cell entry. These findings support the idea that virion-associated cholesterol and sphingolipid may influence viral entry into host cells by altering the interaction between viral particles and a host cell factor(s). Viral entry is a multistep process including binding of the virion to the cell surface and internalization into the cytoplasm by endocytosis. To examine whether virion-associated cholesterol and SM might play a role in cell binding or postbinding events during viral entry, we used a binding assay in which Huh-7 cells preincubated for 1 h at 4°C were infected with B-CD- or SMase-treated HCVcc. Total RNA was extracted after a 1-h addition of the virions at 4°C, followed by quantification of HCV RNA. As shown in Fig. 3A, treatment of the virions with either B-CD or SMase had little influence on their ability to bind to cells.

It has been shown that CD81 plays an important role in HCV internalization but is not correlated with viral attachment (7, 33). An anti-CD81 antibody was used as a negative control for reduced viral attachment. It is likely that heparan sulfate proteoglycan on the target cell surface is needed for the initial attachment of HCV (33). Thus, heparinase I was used as a positive control for reduced HCV attachment to the cells. To examine the roles of cholesterol and sphingolipid on the HCVcc membrane in viral internalization, a virus-cell mixture

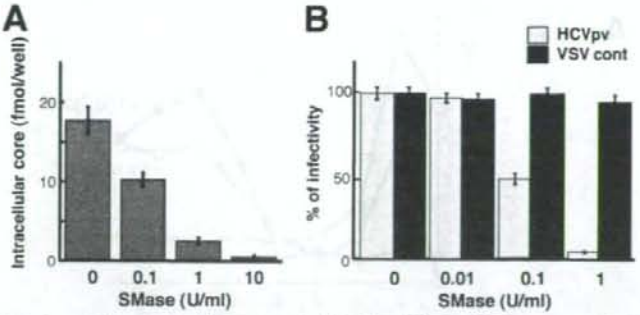

FIG. 2. Effect of SM hydrolysis on viral infectivity. (A) Effect on the infectivity of HCVcc. HCVcc was treated with 0.1, 1, or 10 U/ml SMase for 1 h at 37°C, after which SMase was removed by ultracentifugation. Huh-7 cells were infected with the treated virus, and the core protein content of infected cells was determined at 72 h p.i. (B) Effect on the infectivity of HCVpv (genotype 1a) (shaded bars) or the control, VSVdelG-GFP/G (VSV cont) (solid bars). The viruses were preincubated with SMase for 1 h at 37°C before infection. Data are means from four independent experiments. Error bars, standard deviations.

prepared at 4°C as described above was incubated for 2 h at 37°C, followed by trypsinization to remove virions that were surface bound but not internalized (Fig. 3B). We verified that 94% of surface-bound-viruses were removed by trypsinization using CD81-negative Huh-7 subclones. A marked reduction in viral RNA levels within cells was detected after pretreatment of the virus with either B-CD or SMase. These results strongly suggest that virion-associated cholesterol and sphingolipid function as key determinants of internalization but not of cell attachment.

Association of HCV structural proteins with lipid rafts. Cholesterol and sphingolipid are major components of lipid rafts, which can be isolated as detergent-resistant membranes (DRMs) by treatment with cold TX-100, followed by equilibrium flotation centrifugation. Matto et al. (30) reported that HCV core protein is associated with DRMs in cells carrying the full-length HCV replicon. To investigate whether HCV structural proteins are associated with DRMs in HCVcc-producing cells, lysates from cells infected with HCVcc were subjected to membrane flotation analysis. In the absence of detergent treatment, the majority of the core (Fig. 4A) and E1 (Fig. 4B) proteins were detected in the membrane fractions. After treatment with cold TX-100, significant amounts of both viral proteins were recovered from the DRM fraction. However, after treatment with TX-100 at 37°C, the majority of the E1 and core proteins had shifted to the detergent-soluble fractions. We also found that HCV genotype 1b E1 and E2 can be associated with the lipid raft in 293T cells transfected with an E1 or E2 expression plasmid (Fig. 4C) and that the cytoplasmic tails of envelope

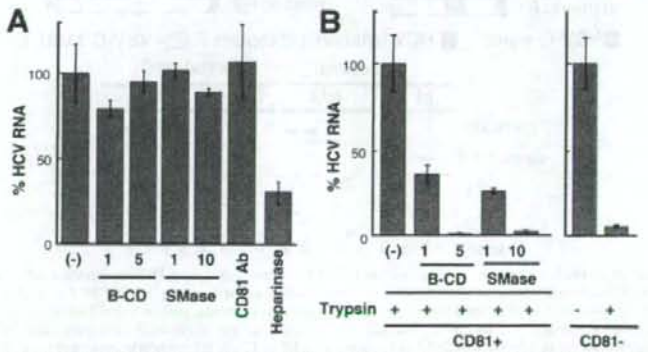

FIG. 3. Effects of B-CD or SMase on virus attachment and internalization. (A) Virus attachment to Huh-7 cells was determined at 4°C after treatment of HCVcc with B-CD (1 or 5 mg/ml) or SMase (1 or 10 U/ml). An antibody (Ab) against CD81 was used, in order to ensure that the antibody did not inhibit HCVcc binding (7, 33). Heparinase was used to reduce HCV attachment to the cell. Viral RNA copies were normalized to total cellular RNA, and the normalized RNA copies in the mock-treated sample (−) were arbitrarily set at 100%. (B) Virus internalization was measured in Huh7-25, a CD81-negative subclone ($CD81^-$) (3), and Huh7-25-CD81, which stably expresses CD81 ($CD81^+$), after treatment of the virions with B-CD or SMase. After internalization for 2 h at 37°C, cells were exposed to trypsin (trypsin +) or phosphate-buffered saline (trypsin −). Huh7-25 was used to ensure that surface-bound virus would be removed by trypsin treatment. The amounts of HCV RNA in Huh7-25 and Huh7-25-CD81 cells infected with untreated HCVcc were assigned the arbitrary value of 100%, respectively. Results are representative of four independent experiments.

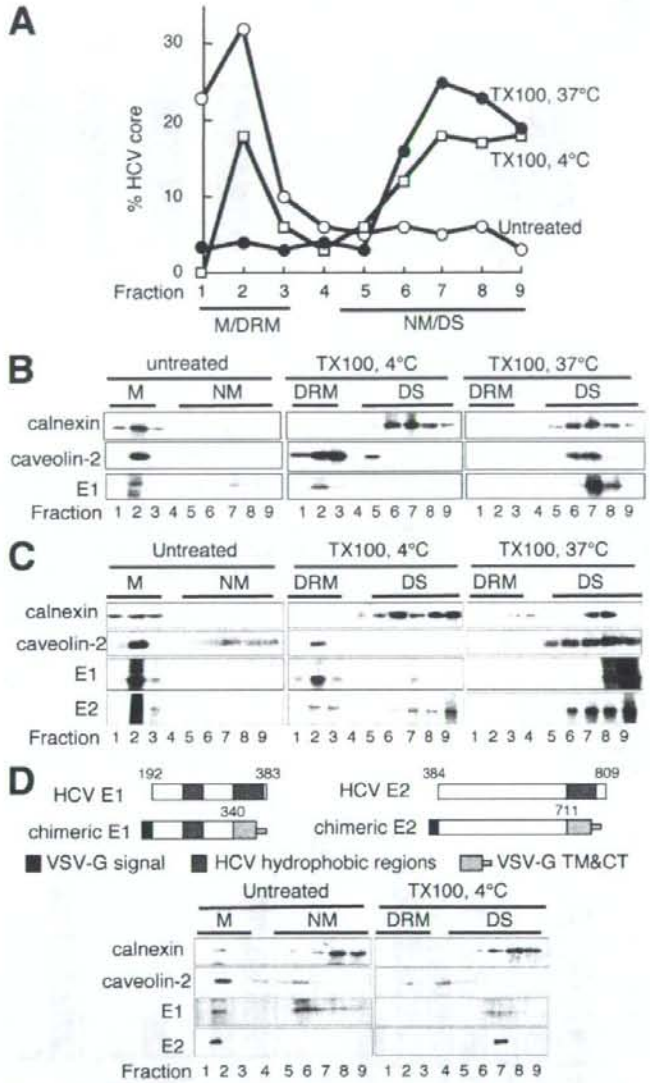

FIG. 4. Compartmentation of HCV structural proteins within DRM fractions. Lysates of HCVcc-infected cells were either treated with 1% TX-100, either on ice or at 37°C, or left untreated, followed by sucrose gradient centrifugation. (A and B) For each fraction, the amount of core protein was determined by an enzyme-linked immunosorbent assay (A), and E1, calnexin, and caveolin-2 were analyzed by Western blotting (B). The amount of core protein in each lysate (TX-100, 37°C; TX-100, 4°C; Untreated) was assigned the arbitrary value of 100%. M, membrane; NM, nonmembrane; DS, detergent soluble. (C) Lysates of 293T cells expressing HCV E1 or E2 protein were either treated with 1% TX-100, either on ice or at 37°C, or left untreated, followed by discontinuous sucrose gradient centrifugation. Each fraction was concentrated in a Centricon YM-30 filter unit and subjected to 12.5% sodium dodecyl sulfate-polyacrylamide gel electrophoresis, followed by immunoblotting with antibodies against calnexin, caveolin-2, Myc (E1), or FLAG (E2). (D) (Top) Structures of HCV envelope genes used. Amino acid positions of HCV are indicated. Signal sequence, transmembrane (TM), and cytoplasmic tail (CT) domains of VSV G protein are shown. (Bottom) Cell lysates expressing chimeric HCV E1 or E2 protein were treated with 1% TX-100 on ice or left untreated, followed by discontinuous sucrose gradient centrifugation. It has been reported that VSV-G is not associated with lipid (39). Calnexin, caveolin-2, and chimeric glycoproteins (chimeric E1 and chimeric E2) were analyzed by immunoblotting. Fractions are numbered from 1 to 9 in order from top to bottom (light to heavy).

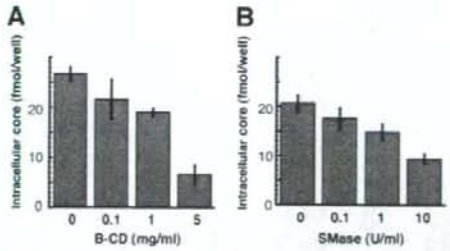

FIG. 5. Effects of B-CD or SMase treatment of cells on HCV infectivity. Huh-7 cells were either left untreated or treated with B-CD at 0.1, 1, or 5 mg/ml (A) or with SMase at 0.1, 1, or 10 U/ml (B) prior to HCVcc infection. Intracellular core levels were quantitated 72 h p.i. Data are means from four independent experiments. Error bars, standard deviations.

proteins are important for their interaction (Fig. 4D). These data suggest that subpopulations of HCV structural proteins are associated with lipid rafts in cells generating the HCV particles.

Moderate inhibition of HCV infection by B-CD or SMase treatment of host cells. It has recently been reported that cholesterol depletion or SM hydrolysis from the host cell membrane decreases HCV infection, in part by decreasing the level of CD81 on the cell surface (19, 53). The involvement of the lipid environment of the host cell plasma membrane in HCV infection was investigated in our HCVcc infection system. Prior to infection, Huh-7 cells were treated with B-CD or SMase and then washed with the medium five times. Cholesterol depletion from Huh-7 cells by B-CD at 1 or 5 mg/ml inhibited HCV core levels by 20 and 75%, respectively, compared to levels in untreated cells (Fig. 5A). We also found that hydrolysis of SM by SMase at 1 or 10 U/ml on the cells, respectively, led to moderate reduction of the viral infection, by 20 or 55% of the infection level of the untreated control (Fig. 5B). There was no influence on cell viability under the conditions of these treatments (data not shown). These findings, compared with the results in Fig. 1A and 2A, suggest that the raft-like environment on the plasma membrane likely serves as a portal for HCV entry, but HCV virion-associated cholesterol and sphingolipid more readily play more critical roles in viral infection.

Inhibitors of the sphingolipid biosynthetic pathway suppress the production of HCVcc, but not RNA replication, for a JFH-1-derived replicon. In the course of studying the involvement of lipid metabolism in the HCV life cycle, we observed that inhibitors of the sphingolipid biosynthetic pathway, including ISP-1 and HPA-12, which specifically inhibit serine palmitoyltransferase (31) and ceramide trafficking from the ER to the Golgi apparatus (55), influenced subgenomic replicons derived from the HCV-N isolate (genotype 1b), but not those derived from JFH-1. A dose-dependent decrease in HCV RNA copy numbers among HCV-N replicon cells was observed upon exposure to ISP-1 or HPA-12, as previously reported (43, 52). In contrast, these compounds had little or no effect on viral RNA accumulation in JFH-1 replicon cells (Fig. 6A). Furthermore, these compounds did not affect luciferase activity in the lysates of Huh-7 cells transfected with an in vitro-transcribed JFH-1 replicon RNA containing a luciferase reporter gene (22) (data not shown). Figure 6B shows the effects of ISP-1 and HPA-12 on de novo sphingolipid biosynthesis by replicon cells. No differences in the inhibitory effects of each compound were observed in replicon cells derived from HCV-N versus JFH-1. When de novo synthesis of sphingolipids was examined by metabolic labeling with [^{14}C]serine, ISP-1 almost completely inhibited the production of both ceramide and SM, while HPA-12 greatly inhibited the synthesis of SM but not ceramide. Levels of phosphatidylethanolamine and phosphatidylserine, into which serine is incorporated by a pathway distinct from that of sphingolipid biosynthesis, were not influenced by these drugs. These results suggest that suppression of HCV RNA replication by inhibitors of sphingolipid biosynthesis might be dependent on the viral genotype or isolate.

This observation prompted us to investigate whether inhibitors of the sphingolipid biosynthetic pathway might have the ability to prevent HCV virion production. Interestingly, when Huh-7 cells producing JFH-1 HCVcc were treated with ISP-1 or HPA-12 under conditions similar to those the replicon cells, viral core levels in the culture supernatants were greatly reduced in a dose-dependent manner. For example, exposure to 10 μM ISP-1 or 1 μM HPA-12 reduced viral core protein levels more than 85% from those for control cells (Fig. 6C). The 50% inhibitory concentrations of both drugs were less than 0.1 μM, 50-fold less than those obtained for the RNA replication of the HCV-N-replicon. Together, these results suggest that the sphingolipid biosynthetic pathway plays an important role in the production of HCV particles, but not in genome replication, in JFH-1-based HCVcc.

DISCUSSION

In this study, we demonstrated the role of HCV virion-associated cholesterol and sphingolipid in viral infectivity. Although dependence on virion-associated cholesterol for virus entry has been shown for a number of viruses (4, 6, 28, 49), this is the first study to demonstrate the importance of envelope cholesterol in a virus belonging to the family *Flaviviridae*. Furthermore, to our knowledge, the functional role of virion membrane-associated SM has not been examined in viruses. Our previous studies using Chinese hamster ovary cell mutants deficient in SM synthesis have demonstrated that reduction of cellular SM levels enhances cellular cholesterol efflux in the presence of B-CD (9, 12). Thus, it may be possible that SM plays a role in the retention of cholesterol on HCV particles due to interaction between cholesterol and SM. The finding that B-CD or SMase treatment of HCVcc markedly inhibited virus internalization but not cell attachment (Fig. 3) suggests that HCV membrane-associated cholesterol and sphingolipid are crucial for the interaction of viral glycoproteins with the virus-receptor/coreceptor required for cell entry. Cholesterol depletion or sphingolipid hydrolysis might induce a conformational change in the viral envelope, resulting in instability of the virion structure. Since the cholesterol/phospholipid ratios of membranes affect bilayer fluidity, the maturation of viral envelopes with high cholesterol/phospholipid ratios via association with rafts may be important for the stability of HCV

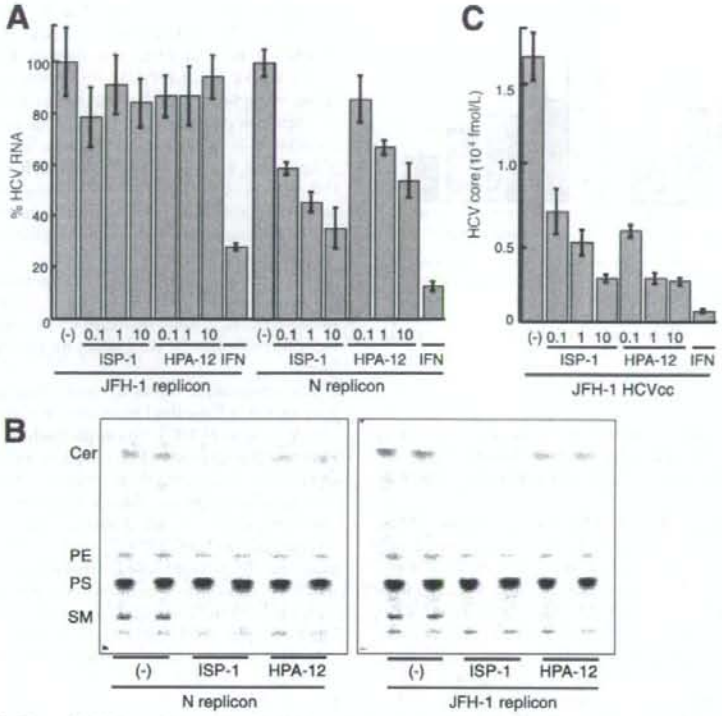

FIG. 6. Anti-HCV effects of inhibitors of the sphingolipid biosynthetic pathway. Subgenomic replicon cells derived from HCV isolate N or JFH-1, as well as HCVcc-producing cells, were treated with ISP-1 (0.1, 1, or 10 μM), HPA-12 (0.1, 1, or 10 μM) or alpha interferon (IFN) (100 U/ml) for 72 h. HCV RNA titers in the replicon cells (A) and the HCV core protein content of the culture medium of infected cells (C) were determined. Data are means from four independent experiments. Error bars, standard deviations. (B) De novo synthesis of sphingolipid in the absence or presence of ISP-1 (10 μM) and HPA-12 (10 μM) was monitored in duplicate by metabolic labeling with [^{14}C]serine for 2 h at 37°C. Cer, ceramide; PE, phosphatidylethanolamine; PS, phosphatidylserine.

particles. Replenishing the viral membrane with cholesterol following treatment with 5 mg/ml B-CD successfully restored viral infectivity to the same level as that of untreated virus (Fig. 1), suggesting that reversible B-CD-induced changes in HCV structure might critically influence viral infectivity. However, we were unable to restore viral infectivity by replenishing cholesterol after pretreatment of the virion with concentrations of B-CD exceeding 10 mg/ml (data not shown). Under these conditions, it is likely that large holes in the viral membrane destroy the virus, a result that cannot be reversed by supplying exogenous cholesterol.

How are cholesterol and sphingolipid involved in the HCV virion during the process of virus maturation? Like most positive-stranded RNA viruses, HCV is thought to assemble at the ER membrane. However, Miyanari et al. (32) reported that lipid droplets are important for HCVcc formation. These authors have shown that the characteristics of lipid-droplet-associated membranes in Huh-7 cells differ from those of ER membranes. In the case of flaviviruses, for which the mechanism of viral assembly and budding remains unclear (15), a few studies have demonstrated budding at the plasma membrane (13, 36, 37, 41), and it has been proposed that the site of budding may be virus and cell type dependent (27). We demonstrate here that subpopulations of HCV structural proteins partition into cellular detergent-resistant, lipid-raft-like membrane fractions in HCVcc-producing cells (Fig. 4) and that inhibitors of the sphingolipid biosynthetic pathway block HCV virion production (Fig. 6). Furthermore, a large proportion of HCV E2 protein incorporated into HCVcc is endoglycosidase H resistant (data not shown). Thus, membrane compartments containing cholesterol- and sphingolipid-rich microdomains may be involved in HCV virion maturation. Another explanation for the recruitment of these lipids to the HCV membrane may be an association between the virus and very-low-density lipoprotein (VLDL) or low-density lipoprotein. Recently, Huang et al. (16) demonstrated a close link between HCV production and VLDL assembly, suggesting that an HCV-VLDL complex is generated and secreted from cells.

Recent reports have demonstrated that CD81-mediated HCV infection is partly dependent on cell membrane choles-

terol (19) and SM (53). We further characterized the role of lipid on the plasma membrane in viral infectivity and found that cholesterol depletion by B-CD, as well as hydrolysis of SM by SMase, moderately inhibits HCV infectivity (Fig. 5). These results suggest that cholesterol and sphingolipid in the plasma membrane environment may assist HCV entry, while HCV virion-associated cholesterol and sphingolipid appear to play critical roles in viral infection.

We previously demonstrated that HCV RNA and nonstructural proteins are present in DRM structures, likely in the context of a lipid-raft structure, and that viral RNA is likely synthesized at a raft membrane structure in cells containing the genotype 1b HCV replicon (2, 10, 46). Here we observed that ISP-1 and HPA-12 suppress HCVcc production, but not viral RNA replication, by the JFH-1 replicon (Fig. 6). Impairment of particle assembly and maturation, rather than suppression of genome replication, by these drugs may account for the inhibition of HCV production in the JFH-1 system. Viral RNA replication of the HCV-N replicon, however, was efficiently inhibited by these compounds, as found in previous reports (43). The virus strain specificity of the anti-HCV activity of cyclosporine has recently been demonstrated: JFH-1 replication is less sensitive to cyclosporine than replication of genotype 1b strains. Furthermore, the requirement for interaction with a cellular replication cofactor, cyclophilin B, differs among HCV strains (18). It appears that ISP-1 and HPA-12 are further examples of diverse effects on HCV strain replication.

In summary, our data here demonstrate important roles of cholesterol and sphingolipid in HCV infection and virion maturation. Specifically, mature HCV particles are rich in cholesterol. Depletion from HCV or hydrolysis of virion-associated SM results in a loss of infectivity. Moreover, the addition of exogenous cholesterol restores infectivity. In addition, cholesterol and sphingolipid on the HCV membrane play key roles in virus internalization, and portions of structural proteins are localized at lipid-raft-like membrane structures within cells. Finally, inhibitors of the sphingolipid biosynthetic pathway efficiently block virion production. These observations suggest that agents capable of modifying virion-associated lipid content might function as antivirals by preventing and/or blocking HCV infection and production.

ACKNOWLEDGMENTS

We thank M. Matsuda, M. Sasaki, S. Yoshizaki, T. Shimoji, M. Kaga, and T. Date for technical assistance and T. Mizoguchi for secretarial work.

This work was partially supported by a grant-in-aid for Scientific Research from the Japan Society for the Promotion of Science, from the Ministry of Health, Labor, and Welfare of Japan, and from the Ministry of Education, Culture, Sports, Science, and Technology, as well as by a Research on Health Science Focusing on Drug Innovation grant from the Japan Health Sciences Foundation.

REFERENCES

1. **Aizaki, H., Y. Aoki, T. Harada, K. Ishii, T. Suzuki, S. Nagamori, G. Toda, Y. Matsuura, and T. Miyamura.** 1998. Full-length complementary DNA of hepatitis C virus genome from an infectious blood sample. Hepatology **27:** 621–627.
2. **Aizaki, H., K. J. Lee, V. M. Sung, H. Ishiko, and M. M. Lai.** 2004. Characterization of the hepatitis C virus RNA replication complex associated with lipid rafts. Virology **324:**450–461.
3. **Akazawa, D., T. Date, K. Morikawa, A. Murayama, M. Miyamoto, M. Kaga, H. Barth, T. F. Baumert, J. Dubuisson, and T. Wakita.** 2007. CD81 expression is important for the permissiveness of Huh7 cell clones for heterogeneous hepatitis C virus infection. J. Virol. **81:**5036–5045.
4. **Bender, F. C., J. C. Whitbeck, H. Lou, G. H. Cohen, and R. J. Eisenberg.** 2005. Herpes simplex virus glycoprotein B binds to cell surfaces independently of heparan sulfate and blocks virus entry. J. Virol. **79:**11588–11597.
5. **Blanchard, E., D. Brand, S. Trassard, A. Goudeau, and P. Roingeard.** 2002. Hepatitis C virus-like particle morphogenesis. J. Virol. **76:**4073–4079.
6. **Chazal, N., and D. Gerlier.** 2003. Virus entry, assembly, budding, and membrane rafts. Microbiol. Mol. Biol. Rev. **67:**226–237.
7. **Evans, M. J., T. von Hahn, D. M. Tscherne, A. J. Syder, M. Panis, B. Wolk, T. Hatziioannou, J. A. McKeating, P. D. Bieniasz, and C. M. Rice.** 2007. Claudin-1 is a hepatitis C virus co-receptor required for a late step in entry. Nature **446:**801–805.
8. **Ezelle, H. J., D. Markovic, and G. N. Barber.** 2002. Generation of hepatitis C virus-like particles by use of a recombinant vesicular stomatitis virus vector. J. Virol. **76:**12325–12334.
9. **Fukasawa, M., M. Nishijima, H. Itabe, T. Takano, and K. Hanada.** 2000. Reduction of sphingomyelin level without accumulation of ceramide in Chinese hamster ovary cells affects detergent-resistant membrane domains and enhances cellular cholesterol efflux to methyl-β-cyclodextrin. J. Biol. Chem. **275:**34028–34034.
10. **Gao, L., H. Aizaki, J. W. He, and M. M. Lai.** 2004. Interactions between viral nonstructural proteins and host protein hVAP-33 mediate the formation of hepatitis C virus RNA replication complex on lipid raft. J. Virol. **78:**3480–3488.
11. **Guo, J. T., V. V. Bichko, and C. Seeger.** 2001. Effect of alpha interferon on the hepatitis C virus replicon. J. Virol. **75:**8516–8523.
12. **Hanada, K., T. Hara, M. Fukasawa, A. Yamaji, M. Umeda, and M. Nishijima.** 1998. Mammalian cell mutants resistant to a sphingomyelin-directed cytolysin. Genetic and biochemical evidence for complex formation of the LCB1 protein with the LCB2 protein for serine palmitoyltransferase. J. Biol. Chem. **273:**33787–33794.
13. **Hase, T., P. L. Summers, K. H. Eckels, and W. B. Baze.** 1987. An electron and immunoelectron microscopic study of dengue-2 virus infection of cultured mosquito cells: maturation events. Arch. Virol. **92:**273–291.
14. **Heider, J. G., and R. L. Boyett.** 1978. The picomole determination of free and total cholesterol in cells in culture. J. Lipid Res. **19:**514–518.
15. **Heinz, F. X., and S. L. Allison.** 2003. Flavivirus structure and membrane fusion. Adv. Virus Res. **59:**63–97.
16. **Huang, H., F. Sun, D. M. Owen, W. Li, Y. Chen, M. Gale, and J. Ye.** 2007. Hepatitis C virus production by human hepatocytes dependent on assembly and secretion of very low-density lipoproteins. Proc. Natl. Acad. Sci. USA **104:**5848–5853.
17. **Ikeda, M., M. Yi, K. Li, and S. M. Lemon.** 2002. Selectable subgenomic and genome-length dicistronic RNAs derived from an infectious molecular clone of the HCV-N strain of hepatitis C virus replicate efficiently in cultured Huh7 cells. J. Virol. **76:**2997–3006.
18. **Ishii, N., K. Watashi, T. Hishiki, K. Goto, D. Inoue, M. Hijikata, T. Wakita, N. Kato, and K. Shimotohno.** 2006. Diverse effects of cyclosporine on hepatitis C virus strain replication. J. Virol. **80:**4510–4520.
19. **Kapadia, S. B., H. Barth, T. Baumert, J. A. McKeating, and F. V. Chisari.** 2007. Initiation of hepatitis C virus infection is dependent on cholesterol and cooperativity between CD81 and scavenger receptor B type I. J. Virol. **81:**374–383.
20. **Kato, T., A. Furusaka, M. Miyamoto, T. Date, K. Yasui, J. Hiramoto, K. Nagayama, T. Tanaka, and T. Wakita.** 2001. Sequence analysis of hepatitis C virus isolated from a fulminant hepatitis patient. J. Med. Virol. **64:**334–339.
21. **Kato, T., T. Date, M. Miyamoto, A. Furusaka, K. Tokushige, M. Mizokami, and T. Wakita.** 2003. Efficient replication of the genotype 2a hepatitis C virus subgenomic replicon. Gastroenterology **125:**1808–1817.
22. **Kato, T., T. Date, M. Miyamoto, M. Sugiyama, Y. Tanaka, E. Orito, T. Ohno, K. Sugihara, I. Hasegawa, K. Fujiwara, K. Ito, A. Ozasa, M. Mizokami, and T. Wakita.** 2005. Detection of anti-hepatitis C virus effects of interferon and ribavirin by a sensitive replicon system. J. Clin. Microbiol. **43:**5679–5684.
23. **Kato, T., T. Date, A. Murayama, K. Morikawa, D. Akazawa, and T. Wakita.** 2006. Cell culture and infection system for hepatitis C virus. Nat. Protoc. **1:**2334–2339.
24. **Kobayashi, S, K. Kakumoto, and M. Sugiura.** 2002. Transition metal salts-catalyzed aza-Michael reactions of enones with carbamates. Org. Lett. **18:** 1319–1322.
25. **Koutsoudakis, G., E. Herrmann, S. Kallis, R. Bartenschlager, and T. Pietschmann.** 2007. The level of CD81 cell surface expression is a key determinant for productive entry of hepatitis C virus into host cells. J. Virol. **81:**588–598.
26. **Lohmann, V., F. Korner, J. Koch, U. Herian, L. Theilmann, and R. Bartenschlager.** 1999. Replication of subgenomic hepatitis C virus RNAs in a hepatoma cell line. Science **285:**110–113.
27. **Mackenzie, J. M., and E. G. Westaway.** 2001. Assembly and maturation of the flavivirus Kunjin virus appear to occur in the rough endoplasmic reticulum and along the secretory pathway, respectively. J. Virol. **75:**10787–10799.
28. **Manes, S., G. del Real, R. A. Lacalle, P. Lucas, C. Gomez-Mouton, S. Sanchez-Palomino, R. Delgado, J. Alcami, E. Mira, and A. C. Martinez.**

2000. Membrane raft microdomains mediate lateral assemblies required for HIV-1 infection. EMBO 1:190–196.
29. **Matsuo, E., H. Tani, C. Lim, Y. Komoda, T. Okamoto, H. Miyamoto, K. Moriishi, S. Yagi, A. H. Patel, T. Miyamura, and Y. Matsuura.** 2006. Characterization of HCV-like particles produced in a human hepatoma cell line by a recombinant baculovirus. Biochem. Biophys. Res. Commun. **340:**200–208.
30. **Matto, M., C. M. Rice, B. Aroeti, and J. S. Glenn.** 2004. Hepatitis C virus core protein associates with detergent-resistant membranes distinct from classical plasma membrane rafts. J. Virol. **78:**12047–12053.
31. **Miyake, Y., Y. Kozutsumi, S. Nakamura, T. Fujita, and T. Kawasaki.** 1995. Serine palmitoyltransferase is the primary target of a sphingosine-like immunosuppressant, ISP-1/myriocin. Biochem. Biophys. Res. Commun. **211:**396–403.
32. **Miyanari, Y., K. Atsuzawa, N. Usuda, K. Watashi, T. Hishiki, M. Zayas, R. Bartenschlager, T. Wakita, M. Hijikata, and K. Shimotohno.** 2007. The lipid droplet is an important organelle for hepatitis C virus production. Nat. Cell Biol. **9:**1089–1097.
33. **Morikawa, K., Z. Zhao, T. Date, M. Miyamoto, A. Murayama, D. Akazawa, J. Tanabe, S. Sone, and T. Wakita.** 2007. The roles of CD81 and glycosaminoglycans in the adsorption and uptake of infectious HCV particles. J. Med. Virol. **79:**714–723.
34. **Murakami, K., K. Ishii, Y. Ishihara, S. Yoshizaki, K. Tanaka, Y. Gotoh, H. Aizaki, M. Kohara, H. Yoshioka, Y. Mori, N. Manabe, I. Shoji, T. Sata, R. Bartenschlager, Y. Matsuura, T. Miyamura, and T. Suzuki.** 2006. Production of infectious hepatitis C virus particles in three-dimensional cultures of the cell line carrying the genome-length dicistronic viral RNA of genotype 1b. Virology **351:**381–392.
35. **Nakai, K., T. Okamoto, T. Kimura-Someya, K. Ishii, C. K. Lim, H. Tani, E. Matsuo, T. Abe, Y. Mori, T. Suzuki, T. Miyamura, J. H. Nunberg, K. Moriishi, and Y. Matsuura.** 2006. Oligomerization of hepatitis C virus core protein is crucial for interaction with the cytoplasmic domain of E1 envelope protein. J. Virol. **80:**11265–11273.
36. **Ng, M. L., J. Howe, V. Sreenivasan, and J. J. Mulders.** 1994. Flavivirus West Nile (Sarafend) egress at the plasma membrane. Arch. Virol. **137:**303–313.
37. **Ng, M. L., S. H. Tan, and J. J. Chu.** 2001. Transport and budding at two distinct sites of visible nucleocapsids of West Nile (Sarafend) virus. J. Med. Virol. **65:**758–764.
38. **Niwa, H., K. Yamamura, and J. Miyazaki.** 1991. Efficient selection for high-expression transfectants with a novel eukaryotic vector. Gene **108:**193–199.
39. **Pessin, J. E., and M. Glaser.** 1980. Budding of Rous sarcoma virus and vesicular stomatitis virus from localized lipid regions in the plasma membrane of chicken embryo fibroblasts. J. Biol. Chem. **255:**9044–9050.
40. **Pitha, J., T. Irie, P. B. Sklar, and J. S. Nye.** 1988. Drug solubilizers to aid pharmacologists: amorphous cyclodextrin derivatives. Life Sci. **43:**493–502.
41. **Rahman, S., T. Matsumura, K. Masuda, K. Kanemura, and T. Fukunaga.** 1998. Maturation site of dengue type 2 virus in cultured mosquito C6/36 cells and Vero cells. Kobe J. Med. Sci. **44:**65–79.
42. **Rouser, G., G. Galli, and G. Kritchevsky.** 1967. Lipid composition of the normal human brain and its variations during various diseases. Pathol. Biol. **15:**195–200.
43. **Sakamoto, H., K. Okamoto, M. Aoki, H. Kato, A. Katsume, A. Ohta, T. Tsukuda, N. Shimma, Y. Aoki, M. Arisawa, M. Kohara, and M. Sudoh.** 2005. Host sphingolipid biosynthesis as a target for hepatitis C virus therapy. Nat. Chem. Biol. **1:**333–337.
44. **Sato, K., H. Okamoto, S. Aihara, Y. Hoshi, T. Tanaka, and S. Mishiro.** 1993. Demonstration of sugar moiety on the surface of hepatitis C virions recovered from the circulation of infected humans. Virology **196:**354–357.
45. **Serafino, A., M. B. Valli, F. Andreola, A. Crema, G. Ravagnan, L. Bertolini, and G. Carloni.** 2003. Suggested role of the Golgi apparatus and endoplasmic reticulum for crucial sites of hepatitis C virus replication in human lymphoblastoid cells infected in vitro. J. Med. Virol. **70:**31–41.
46. **Shi, S. T., K. J. Lee, H. Aizaki, S. B. Hwang, and M. M. Lai.** 2003. Hepatitis C virus RNA replication occurs on a detergent-resistant membrane that cofractionates with caveolin-2. J. Virol. **77:**4160–4168.
47. **Shinitzky, M., and M. Inbar.** 1976. Microviscosity parameters and protein mobility in biological membranes. Biochim. Biophys. Acta **433:**133–149.
48. **Shirakura, M., K. Murakami, T. Ichimura, R. Suzuki, T. Shimoji, K. Fukuda, K. Abe, S. Sato, M. Fukasawa, Y. Yamakawa, M. Nishijima, K. Moriishi, Y. Matsuura, T. Wakita, T. Suzuki, P. M. Howley, T. Miyamura, and I. Shoji.** 2007. E6AP ubiquitin ligase mediates ubiquitylation and degradation of hepatitis C virus core protein. J. Virol. **81:**1174–1185.
49. **Stuart, A. D., H. E. Eustace, T. A. McKee, and T. D. Brown.** 2002. A novel cell entry pathway for a DAF-using human enterovirus is dependent on lipid rafts. J. Virol. **76:**9307–9322.
50. **Takikawa, S., K. Ishii, H. Aizaki, T. Suzuki, H. Asakura, Y. Matsuura, and T. Miyamura.** 2000. Cell fusion activity of hepatitis C virus envelope proteins. J. Virol. **74:**5066–5074.
51. **Tani, H., Y. Komoda, E. Matsuo, K. Suzuki, I. Hamamoto, T. Yamashita, K. Moriishi, K. Fujiyama, T. Kanto, N. Hayashi, A. Owsianka, A. H. Patel, M. A. Whitt, and Y. Matsuura.** 2007. Replication-competent recombinant vesicular stomatitis virus encoding hepatitis C virus envelope proteins. J. Virol. **81:**8601–8612.
52. **Umehara, T., M. Sudoh, F. Yasui, C. Matsuda, Y. Hayashi, K. Chayama, and M. Kohara.** 2006. Serine palmitoyltransferase inhibitor suppresses HCV replication in a mouse model. Biochem. Biophys. Res. Commun. **346:**67–73.
53. **Voisset, C., M. Lavie, F. Helle, A. Op De Beeck, A. Bilheu, J. Bertrand-Michel, F. Tercé, L. Cocquerel, C. Wychowski, N. Vu-Dac, and J. Dubuisson.** 2008. Ceramide enrichment of the plasma membrane induces CD81 internalization and inhibits hepatitis C virus entry. Cell. Microbiol. **10:**606–617.
54. **Wakita, T., T. Pietschmann, T. Kato, T. Date, M. Miyamoto, Z. Zhao, K. Murthy, A. Habermann, H. G. Krausslich, M. Mizokami, R. Bartenschlager, and T. J. Liang.** 2005. Production of infectious hepatitis C virus in tissue culture from a cloned viral genome. Nat. Med. **11:**791–796.
55. **Yasuda, S., H. Kitagawa, M. Ueno, H. Ishitani, M. Fukasawa, M. Nishijima, S. Kobayashi, and K. Hanada.** 2001. A novel inhibitor of ceramide trafficking from the endoplasmic reticulum to the site of sphingomyelin synthesis. J. Biol. Chem. **276:**43994–44002.
56. **Zhong, J., P. Gastaminza, G. Cheng, S. Kapadia, T. Kato, D. R. Burton, S. F. Wieland, S. L. Uprichard, T. Wakita, and F. V. Chisari.** 2005. Robust hepatitis C virus infection in vitro. Proc. Natl. Acad. Sci. USA **102:**9294–9299.

JOURNAL OF VIROLOGY, Apr. 2008, p. 3480–3489 Vol. 82, No. 7
0022-538X/08/$08.00+0 doi:10.1128/JVI.02253-07

A Single-Amino-Acid Mutation in Hepatitis C Virus NS5A Disrupting FKBP8 Interaction Impairs Viral Replication▽

Toru Okamoto,[1] Hiroko Omori,[2] Yuuki Kaname,[1] Takayuki Abe,[1] Yorihiro Nishimura,[3] Tetsuro Suzuki,[3] Tatsuo Miyamura,[3] Tamotsu Yoshimori,[2] Kohji Moriishi,[1] and Yoshiharu Matsuura[1]*

Department of Molecular Virology[1] and Department of Cellular Regulation,[2] Research Institute for Microbial Diseases, Osaka University, Osaka, and Department of Virology II, National Institute of Infectious Diseases, Tokyo,[3] Japan

Received 17 October 2007/Accepted 16 January 2008

Hepatitis C virus (HCV) nonstructural protein 5A (NS5A) regulates viral replication through its interaction with host and other viral proteins. We have previously shown that FK506-binding protein 8 (FKBP8) binds to NS5A and recruits Hsp90 to form a complex that participates in the replication of HCV. In this study, we examined the biochemical characteristics of the interaction and the intracellular localization of NS5A and FKBP8. Surface plasmon resonance analysis revealed that the dissociation constant of the interaction between the purified FKBP8 and NS5A expressed in bacteria was 82 nM. Mutational analyses of NS5A revealed that a single amino acid residue of Val or Ile at position 121, which is well conserved among all genotypes of HCV, is critical for the specific interaction with FKBP8. Substitution of the Val^{121} to Ala drastically impaired the replication of HCV replicon cells, and the drug-resistant replicon cells emerging after drug selection were shown to have reverted to the original arrangement by replacing Ala^{121} with Val. Examination of individual fields of the replicon cells by both fluorescence microscopy and electron microscopy (the correlative fluorescence microscopy-electron microscopy technique) revealed that FKBP8 is partially colocalized with NS5A in the cytoplasmic structure known as the membranous web. These results suggest that specific interaction of NS5A with FKBP8 in the cytoplasmic compartment plays a crucial role in the replication of HCV.

Hepatitis C virus (HCV) infects more than 170 million people worldwide, a large percentage of whom suffer from persistent infection and severe chronic liver diseases, culminating in cirrhosis and hepatocellular carcinoma (51). Combination therapy with pegylated interferon (IFN) and ribavirin achieves a 40 to 50% sustained virological response in patients infected with genotype 1 HCV (30). Recently, therapeutics have been developed to target the protease and polymerase of HCV, as well as the host factors required for the viral replication (24, 42).

HCV belongs to the *Flaviviridae* family and has a single-stranded positive-sense RNA genome with a nucleotide length of 9.6 kb. The viral genome, translation of which depends on its own internal ribosomal entry site found within the 5′ nontranslated region, encodes a large precursor protein composed of about 3,000 amino acids. The polyprotein is cleaved by host and viral proteases, resulting in viral structural proteins (core, E1, and E2), a putative viropore protein (p7), and nonstructural proteins (NS2, NS3, NS4A, NS4B, NS5A, and NS5B) (33). In the last decade, the mechanism by which HCV replicates in the hepatoma cell line Huh-7 has been partially revealed in studies using a cell culture system. The HCV replicon system, which encompasses the autonomously replicable genome of HCV in the Huh-7 cell line or other cell lines derived from it, has been established to accumulate information about the mechanism of HCV replication and to be utilized for screening antiviral drug candidates (27). In addition, the cell culture system for the propagation of infectious HCV particles was developed by using a full-length genome of HCV genotype 2a, JFH1 virus, which was isolated from a fulminant hepatitis C patient (25, 49, 57). However, a robust cell culture system for HCV of genotypes 1a and 1b, the most prevalent genotypes in the world, has not yet been successfully developed, with the exception of the cell culture systems for strains H77 and H77-S of the 1a genotype (21, 56). Furthermore, it is currently impossible to obtain a sufficient amount of HCV particles for biological and physiochemical studies due to the low viral load in the sera of hepatitis C patients and the low yield of HCV particles in the present cell culture system.

HCV NS5A is a membrane-anchored phosphoprotein that appears to possess multiple and diverse functions in viral replication, as well as in the establishment and maintenance of persistent infection (29, 38). Structural analyses suggest that NS5A forms a dimer and has a zinc-binding motif required for replication in the N-terminal domain (45, 46). NS5A has the IFN sensitivity-determining and MyD88-binding regions in the central domain (1, 10), and the SH3-binding region and nuclear localization signal in the C-terminal domain (28, 29). Adaptive mutations of NS5A have frequently been found in the replicon cells exhibiting efficient replication (4, 55). Several host proteins and lipids have been reported to interact with NS5A to upregulate the viral replication. For example, HCV replication was inhibited by treatment with lovastatin, an inhibitor of 3-hydroxy-3-methylglutaryl coenzyme A reductase, and this inhibition was restored by the addition of geranylgeraniol, suggesting that HCV replication requires geranylgera-

* Corresponding author. Mailing address: Department of Molecular Virology, Research Institute for Microbial Diseases, Osaka University, 3-1, Yamadaoka, Suita-shi, Osaka 565-0871, Japan. Phone: 81-6-6879-8340. Fax: 81-6-6879-8269. E-mail: matsuura@biken.osaka-u.ac.jp.

▽ Published ahead of print on 23 January 2008.

nylated proteins (22, 54). In addition, the F-box and leucine-rich repeat protein 2 (FBL2) was identified as a binding partner of NS5A, and geranylgeranylation of FBL2 was shown to be required for replication of HCV RNA (50). Vesicle-associated membrane protein (VAMP)-associated protein (VAP) subtype A (VAP-A) and subtype B (VAP-B) were also shown to interact with NS5A and NS5B through the coiled-coil domain and the N-terminal major sperm protein domain, respectively (11, 16, 39).

Immunophilins are known to share the peptidyl prolyl *cis/trans* isomerase activity, thereby basically conserving the ability to interact with immunosuppressive drugs such as cyclosporine and tacrolimus (FK506). Cyclophilin B, one of the cyclosporine-binding immunophilins, can bind to NS5B and upregulate the replication of HCV (53). We have previously reported that NS5A specifically interacts with FK506-binding protein 8 (FKBP8) and recruits heat shock protein 90 (Hsp90) to the viral RNA replication complex through the interaction of the carboxylate clump structure of FKBP8 with the C-terminal MEEVD motif of Hsp90 (37). Knockdown of FKBP8 reduced the replication efficiency of the HCV genome in the replicon cells and the cells infected with JFH1 virus (37), suggesting that FKBP8 is required for the replication of HCV via formation of the replication complex. In the present study we identified an amino acid residue in NS5A responsible for specific interaction with FKBP8 and examined the biochemical interaction and intracellular localization of NS5A and FKBP8.

MATERIALS AND METHODS

Cells. Human embryo kidney 293T cells, and human hepatoma cell line Huh-7 and its derivatives were maintained in Dulbecco modified Eagle medium (DMEM; Sigma, St. Louis, MO) containing 10% fetal calf serum (FCS) and nonessential amino acid (NEAA). The Huh-7 9-13 cell line, which harbors an HCV subgenomic replicon (4, 27), was cultured in DMEM supplemented with 10% FCS and 1 mg of G418 and NEAA/ml. The Huh-7 9-13 cell line was treated with IFN-α to deplete the HCV RNA replicon. A cell line exhibiting the highest efficiency of propagation of JFH1 virus was selected by limited dilution and designated Huh-7OK1. The Huh-7OK1 cell line retained the ability to produce type I IFNs through the RIG-I-dependent signaling pathway upon infection with RNA viruses and exhibited a cell surface expression level of human CD81 comparable to that of the parental cell line. Detailed characteristics of this cell line are described elsewhere.

Antibodies. Rabbit antibody to NS5A was prepared by immunization with the NS5A peptide as described previously (16). Mouse monoclonal antibody to NS5A was purchased from Austral Biologicals (San Ramon, CA). Mouse monoclonal antibody to FKBP8 (KDM11) was described previously (37).

Plasmids. cDNA encoding NS5A was amplified from the HCV genotype 1b Con1 strain, kindly provided by R. Bartenschlager, by PCR using *Pfu* Turbo DNA polymerase (Stratagene, La Jolla, CA). The DNA fragment was cloned into pCAGGs-PUR/N-HA (36, 37). Human FKBP8 cDNA was amplified from the total cDNA of Huh-7 cells by PCR, and the fragment was introduced into pcDNA3.1 N-Flag, in which a Flag tag is introduced in the 5′ terminus of the cloning site of pcDNA3.1(+) (Invitrogen, Carlsbad, CA). The point mutations of NS5A were generated by the method of splicing by overlap extension (17, 18) and introduced into pCAGGs-PUR/N-HA. The mutant NS5A cDNAs were amplified by PCR, digested with MluI and XhoI, and introduced into the replicon plasmid pFKI$_{neo}$/neo/NS3-3′/5.1 (23), provided by R. Bartenschlager, or pFKI$_{neo}$/hRL/NS3-3′/5.1 (37). The cDNA encoding NS3 to NS5A was excised from pFKI$_{neo}$/neo/NS3-3′/5.1 and cloned into pCAGGs-PUR (36, 37). pET-UbCHis-del32-NS5A encoding an NS5A lacking the membrane-anchoring region (amino acid residues 1 to 32) and *Escherichia coli* strain BL21(DE3)/pCG1 was kindly provided by C. E. Cameron (19). The DNA fragment encoding the regions spanning from amino acid residues 2 to 389 of FKBP8 lacking the transmembrane region was amplified by PCR and replaced with the NS5A coding region of pET-UbNHis-del32-NS5A. The resulting plasmid encoding the amino acid residues from 2 to 389 of FKBP8 was designated pET-UbNHis-FKBP8(dTM) in this report. The DNA fragment encoding FKBP52 was amplified from the human fetal brain library (Clontech, Palo Alto, CA) by PCR and then was introduced into pET30a (Novagen, San Diego, CA) to be expressed in *E. coli*. The resulting plasmid was designated pET30a-FKBP52. The sequences of the plasmids were confirmed by using an ABI Prism 3130 genetic analyzer (Applied Biosystems, Tokyo, Japan).

Protein purification. The procedure used for protein purification was basically that of Huang et al. (19), with minor modifications that have been described previously (37). Briefly, overnight culture of *E. coli* strains transformed with pET-UbCHis-del32-NS5A, pET-UbNHis-FKBP8(dTM), or pET30a-FKBP52 were added at 1/100 volume into 250 ml of 2xYT medium and incubated at 37°C with shaking at 200 rpm. IPTG(isopropyl β-D-thiogalactoside) was added at a final concentration of 0.5 mM when the absorbance of the culture reached an optical density at 600 nm of 0.6 to 0.8, and then the culture solution was incubated at 20°C for 4 h with shaking at 200 rpm. After centrifugation of the culture at 3,000 × *g* for 5 min, the pellets were washed once with phosphate-buffered saline (PBS); suspended in 5 ml of 100 mM Tris-HCl (pH 8.0)–200 mM NaCl–10 mM 2-mercaptoethanol (lysis buffer) containing 0.5% Nonidet P-40, EDTA-free complete protease inhibitor (Roche, Indianapolis, IN), and 0.2 μg of lysozyme/ml; incubated at 4°C for 1 h; and subjected to freezing-thawing once. The resulting mixture was sonicated at 4°C for 5 min and was treated with 0.02 mg of DNase per ml at room temperature for 5 min. The suspension was centrifuged at 4°C at 30,000 rpm for 1 h in a Beckman SW50.1 (Beckman Coulter, Fullerton, CA), and the resulting supernatant was mixed with 0.5 ml of nickel agarose (Sigma) and gently rotated at 4°C for 60 min. The nickel resins were washed twice by spinning down with lysis buffer containing 10 mM imidazole. The recombinant protein was eluted from the nickel resin with lysis buffer containing 0.25 M imidazole and then dialyzed in 20 mM Tris-HCl (pH 8.0) containing 100 mM NaCl. The dialyzed eluates were applied to a Resource Q Sepharose column (GE Healthcare, Tokyo, Japan), washed with a ten-column volume of 20 mM Tris-HCl buffer (pH 8.0) containing 100 mM NaCl, and eluted under a linear gradient of 100 to 1,000 mM NaCl in 20 mM Tris-HCl buffer (pH 8.0). The peak fractions were pooled into a tube and concentrated by using Amicon Ultra-4 (Millipore, Bedford, MA). A half volume of the concentrated fraction was dialyzed against 10 mM HEPES (pH 7.4) containing 150 mM NaCl and 3 mM EDTA (HBS-E buffer) for analysis of the binding kinetics, while the remaining half was dialyzed in PBS for the immobilization on the sensor chip and pull-down assay. The protein concentration was measured using a Coomassie protein assay kit (Pierce, Rockford, IL).

Binding kinetics of NS5A and FKBP8. Surface plasmon resonance (SPR) measurements were made at 25°C by using a Bicore 2000 biosensor (GE Healthcare) in accordance with the manufacturer's instructions to determine the affinity between NS5A and FKBP8. Briefly, The NS5A-His was immobilized as ligand on a carboxymethyl-dextran (CM5) sensor chip with an amine coupling kit (Biacore). His-FKBP8 and His-FKBP52 were diluted with HBS-E buffer containing 0.0005% surfactant P20 (HBS-EP buffer) at the concentrations indicated in Fig. 1. The diluted sample was applied to the sensor chip at a flow rate of 20 μl/min in HBS-EP. The raw data were analyzed with a Biaevaluation software package (version 3.0; GE Healthcare).

Immunofluorescence microscopy. Huh-7 9-13 replicon cells cultured on glass slides overnight were fixed with 4% paraformaldehyde in PBS at room temperature for 20 min. After two washes with PBS, cells were permeabilized for 15 min at room temperature with PBS containing 0.25% saponin and blocked with PBS containing 1% bovine serum albumin (PBS-BSA) for 30 min at room temperature. The cells were then incubated with PBS-BSA containing mouse anti-FKBP8 antibody (KDM11) and/or rabbit anti-NS5A antibody at 37°C for 60 min, washed three times with PBS-BSA, and incubated with PBS-BSA containing Alexa Fluor 488 (AF488)-conjugated anti-mouse immunoglobulin G (IgG), AF488-conjugated anti-rabbit IgG, AF594-conjugated anti-rabbit IgG, and/or AF546-conjugated anti-mouse IgG antibody (Molecular Probes, Eugene, OR) at 37°C for 60 min. Finally, the cells were washed three times with PBS-BSA and observed on a FluoView FV1000 laser scanning confocal microscope (Olympus, Tokyo, Japan). For mitochondria and lipid droplet staining, cells were incubated with culture medium containing Mitotracker Deep-Red (200 nM; Molecular Probes) and Bodipy 558/568 C12 (20 μg/ml; Molecular Probes), respectively, for 20 min at 37°C. After staining, cells were washed once with fresh and prewarmed culture medium and incubated at 37°C for 20 min.

Correlative FM-EM. Correlative fluorescence microscopy-electron microscopy (FM-EM) allows individual cells to be examined both in an overview with FM and in a detailed subcellular structure view with EM (40). For the observation by FM-EM, the Huh-7 9-13 replicon or Huh-7OK1 cells were cultured on gridded, 35-mm glass-bottom dishes (Mat Tek, Ashland, MA) in 1 ml of DMEM containing 10% FCS at 37°C overnight. Cells on the grid were fixed and stained

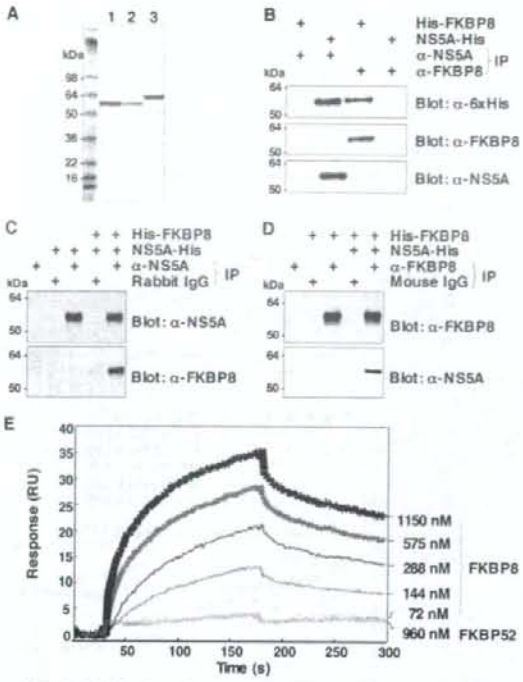

FIG. 1. Purification of recombinant NS5A, FKBP8, and FKBP52 and characteristics of their interaction. (A) Purified recombinant His-FKBP8 (lane 1), NS5A-His (lane 2), and His-FKBP52 (lane 3) were subjected to SDS-PAGE and stained with Coomassie brilliant blue G-250. The molecular size marker is shown on the left. (B) Antibodies to NS5A and FKBP8 specifically precipitated NS5A-His and His-FKBP8, respectively, and exhibit no cross-activity. The purified recombinant proteins (10 μg) were mixed, and immunoprecipitated with rabbit polyclonal IgG to NS5A or nonspecific rabbit IgG (C) or immunoprecipitated with mouse monoclonal antibody to FKBP8 (KDM11) or nonspecific mouse IgG (D). Immunoprecipitated proteins were subjected to immunoblotting with antibodies to NS5A and FKBP8. (E) The kinetics of interaction between His-FKBP8 and NS5A-His was estimated from SPR by using a Biacore 2000. The data are representative of three independent experiments.

with the specific antibodies as described above and then examined by using a confocal laser scanning microscope. The same specimens were then further incubated with 2.5% glutaraldehyde and 2% formaldehyde in PBS at 4°C overnight. After three washings with PBS, the samples were postfixed with 1% osmium tetroxide and 0.5% potassium ferrocyanide in PBS for 1 h, washed with distilled water three times, dehydrated in ethanol, and embedded in Epon812 (Structure Probe, West Chester, PA). Ultrathin sections of the cell (70-nm thick) were stained with saturated uranyl acetate and Reynolds lead citrate solution. The electron micrographs were taken with a JEOL JEM-1011 transmission electron microscope (JEOL, Ltd., Tokyo, Japan).

Transfection, immunoblotting, and immunoprecipitation. The transfection and immunoprecipitation tests were carried out as described previously (37). The immunoprecipitated samples were subjected to sodium dodecyl sulfate (SDS)–12.5 or 10% polyacrylamide gel electrophoresis. The proteins were transferred to polyvinylidene difluoride membranes (Millipore) and reacted with the appropriate antibodies. The immune complexes were visualized with Super Signal West Femto substrate (Pierce) and were detected by using an LAS-3000 image analyzer system (Fujifilm, Tokyo, Japan).

Transient replication assay. The HCV replicon plasmid, pFK-I_{389} hRL/NS3-3'/5.1 (37), was cleaved with ScaI and transcribed in vitro by using a MEGAscript T7 kit (Ambion, Austin, TX). Then, 10 μg of the transcribed RNA was electroporated at 270 V and 960 μF by a Gene Pulser (Bio-Rad, Hercules, CA) into 10 million cells of Huh-7OK1 of cell line per ml, suspended in 25 ml of culture medium, and then seeded at 1 ml per well on 12-well culture plates. Luciferase activity was measured at 4 and 48 h posttransfection using a *Renilla* luciferase assay system (Promega, Madison, WI) according to the manufacturer's protocol. The relative luciferase activity was presented as the ratio of the luciferase activity measured at 48 h posttransfection to that at 4 h.

Colony formation. The plasmid pFK-I_{389} neo/NS3-3'/NK5.1 (23) was digested with ScaI, and 10 μg of the in vitro-transcribed RNA was electroporated onto 4 million Huh-7 cells per 0.4 ml and suspended in 10 ml of the culture medium as described above. A 3-ml aliquot of the resulting cell suspension was mixed with 7 ml of the culture medium and inoculated into a culture dish 10 cm in diameter. The culture medium was replaced with fresh DMEM containing 10% FCS and 1 mg of G418 (Nakarai Tesque, Tokyo, Japan)/ml at 24 h posttransfection. The medium was exchanged once a week with fresh DMEM containing 10% FCS and 1 mg of G418/ml, and the remaining colonies were fixed with 4% paraformaldehyde at 28 days posttransfection and stained with crystal violet.

Direct sequencing of the NS5A gene in a G418-resistant cell line. Total RNA was prepared from G418-resistant colonies by using an RNeasy minikit (Qiagen, Valencia, CA), and first-strand cDNA was synthesized with random primers by using a first-strand cDNA synthesis kit (GE Healthcare). The NS5A genes were amplified with the primer pair 5'-GACGGCATCATGCAAACCAC-3' and 5'-CGTGGAGGTGGTATCGGAGG-3'. The PCR products were applied to agarose gel electrophoresis and purified by using a gel extraction kit (Qiagen). The purified PCR products were sequenced with the inside primer 5'-ATTAACGC GTACACCACGGG-3' by using an ABI Prism 3130 genetic analyzer (Applied Biosystems).

RESULTS

Purification of recombinant NS5A, FKBP8, and FKBP52 and characteristics of their interaction. We have previously reported that the thioredoxin-tagged domain I of NS5A (Trx-NS5A) binds directly to His_6-tagged FKBP8 (37), although we could not obtain sufficient amounts of the recombinant FKBP8 for further biochemical analysis. Huang et al. reported that C-terminally His_6-tagged NS5A lacking the N-terminal 32 amino acid residues of the membrane anchoring region (NS5A-His) could be purified by using a pET-ubiquitin expression system, in which the NS5A-His fused with ubiquitin at the C terminus was cleaved off by a ubiquitin-specific protease, Ubp1, in *E. coli* and then purified by using nickel-charged resin (19). By using the pET-ubiquitin expression system, we could obtain 1 mg of the purified His-FKBP8 protein from 1 liter of a culture of *E. coli* harboring a pET-UbCHis-FKBP8-dTM encoding an N-terminally His_6-tagged FKBP8 lacking the transmembrane region (His-FKBP8), which is five times greater production than that achieved by the previous method we used (37). His-FKBP8, NS5A-His, and His-FKBP52 (10 μg) were purified with nickel-charged resin (Fig. 1A) and subjected to the pull-down assay. Immunoblotting, instead of protein staining, was used for detection of the precipitates due to the similar molecular sizes of NS5A-His and His-FKBP8 (Fig. 1A). To confirm the specificity of the antibodies to NS5A and FKBP8, NS5A-His and His-FKBP8 were immunoprecipitated and then subjected to immunoblotting by the antibodies. The antibodies to NS5A and FKBP8 specifically recognize NS5A and FKBP8, respectively (Fig. 1B). The antibody to NS5A, but not nonspecific rabbit IgG, precipitated NS5A together with FKBP8 (Fig. 1C). The reverse experiment was also successful in demonstrating that antibody to FKBP8, but not nonspecific mouse IgG, precipitated FKBP8 with NS5A (Fig. 1D). The binding kinetics was analyzed on the basis of the SPR technology to examine the specificity of interaction between FKBP8

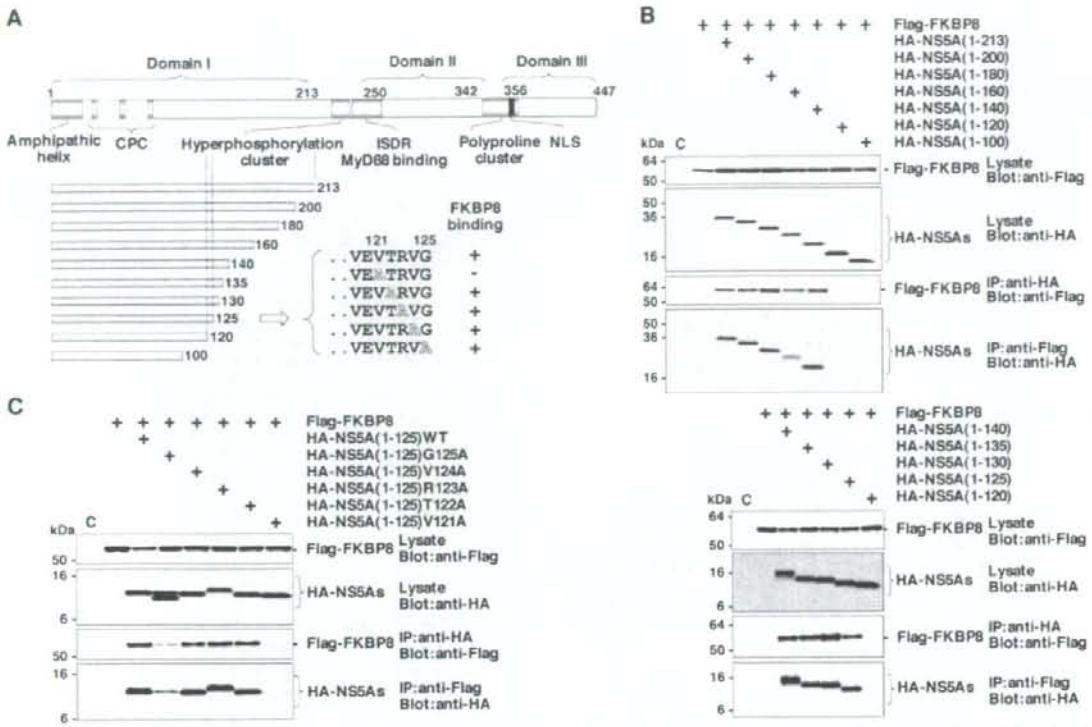

FIG. 2. Determination of an amino acid residue responsible for the interaction of FKBP8 and NS5A domain I. (A) Structure and functional domains of NS5A (top). The C-terminal deletion mutants of HA-tagged NS5A domain I used in the present study. Gray and white bars indicate ability and inability to bind to FKBP8, respectively. The site of Ala substitution of HA-tagged NS5A(1-125) and the results of binding to FKBP8 are summarized on the right. (B) The C-terminal deletion mutants of HA-tagged NS5A domain I were coexpressed with Flag-FKBP8 in 293T cells and immunoprecipitated with anti-HA or anti-Flag antibody. Immunoprecipitates were analyzed by immunoblotting. (C) Five substitution mutants of HA-NS5A(1-125) replacing each of the amino acid residues from 121 to 125 with Ala were coexpressed with Flag-FKBP8 in 293T cells, immunoprecipitated, and analyzed by immunoblotting. The data are representative of three independent experiments.

and NS5A. His-FKBP8 or His-FKBP52 was applied to a flow line at various concentrations on the sensor chip on which NS5A-His was immobilized. Each background signal was determined by flowing the FKBPs over a blank chip. The SPR signal of His-FKBP8 or His-FKBP52 was determined after subtraction by the background signals. The SPR was increased corresponding to the amount of His-FKBP8, but no response was observed with His-FKBP52 (Fig. 1D). The values of the dissociation constant, K_d (10^{-3} s^{-1}), and K_a (10^3 M^{-1} s^{-1}) were calculated to be 1.86 and 22.8, respectively. Therefore, the equilibrium dissociation constant (K_D) of the interaction between His-FKBP8 and NS5A-His was determined as 82 nM, suggesting a specific binding of the proteins. These results indicate that FKBP8 directly and specifically interacts with NS5A.

Val^{121} of NS5A is responsible for the specific interaction with FKBP8. The domain I of NS5A (amino acid residues 1 to 213) was shown to interact with FKBP8 (37). However, further analyses on the specific interaction of NS5A with FKBP8 have not yet been carried out. To determine the amino acid residues in NS5A responsible for specific interaction with FKBP8, Flag-FKBP8 was coexpressed with C-terminal deletion mutants of the hemagglutinin (HA)-tagged NS5A domain I in 293T cells and immunoprecipitated with appropriate antibodies (Fig. 2A). Although the C-terminal deletions up to the residue 141 in HA-NS5A exhibited no effect on the coimmunoprecipitation with Flag-FKBP8, further deletion beyond the amino acid residue 121 of HA-NS5A abrogated the coprecipitation with Flag-FKBP8 (Fig. 2B, upper panel), suggesting that residues from 121 to 140 in NS5A are responsible for the interaction with FKBP8. Further deletion mutants of HA-NS5A revealed that the amino acid residues from 121 to 125 are required for the interaction with Flag-FKBP8 (Fig. 2B, lower panel). To identify a specific amino acid residue critical for interaction with FKBP8, we generated substitution mutants of HA-NS5A(1-125) in which each of the amino acid residues from 121 to 125 were replaced with Ala. The mutant in which Val^{121} was replaced with Ala completely abrogated the interaction of HA-NS5A(1-125) with Flag-FKBP8, but the other substitution mutants did not (Fig. 2C). However, we could not obtain a clear reduction in the interaction of FKBP8 with a full-length of NS5A mutant substituted Val^{121} with Ala by immunoprecipi-

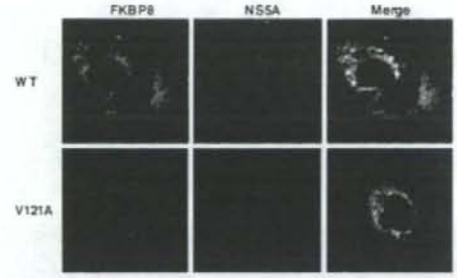

FIG. 3. Intracellular localization of wild-type and V121A mutant NS5A with FKBP8. Huh-7OK1 cells transfected with expression plasmids encoding HCV nonstructural proteins carrying a wild-type (WT) or mutant NS5A substituted Val^{121} with Ala (V121A) were fixed with 4% paraformaldehyde in PBS and permeabilized with 0.25% saponin. Endogenous FKBP8 and NS5A were stained with anti-FKBP8 monoclonal antibody (KDM11) and rabbit anti-NS5A polyclonal antibody, followed by staining with AF488-conjugated anti-mouse IgG and AF594-conjugated anti-rabbit IgG antibodies, respectively.

tation analysis (data not shown). To examine the interaction of NS5A with FKBP8 in more functional setting, we examined the colocalization of the wild-type or mutant NS5A with an endogenous FKBP8 in Huh-7OK1 cells by transfection of the expression plasmids encoding HCV nonstructural proteins carrying a wild-type or mutant NS5A substituted Val^{121} with Ala. As shown in Fig. 3, colocalization of an endogenous FKBP8 with NS5A was reduced by the introduction of substitution of Val^{121} to Ala. These results suggest that Val^{121} of NS5A plays a critical role in the specific interaction with FKBP8.

Effect of the interaction of NS5A with FKBP8 on the replication of HCV. The amino acid alignment of NS5A derived from several genotypes on the basis of the European HCV database (http://euhcvdb.ibcp.fr/euHCVdb/jsp/index.jsp) revealed that the amino acid residue Val^{121} is well conserved among NS5A of various genotypes of HCV, with the exception of the genotype 1a strains, which have Ile in place of Val (Fig. 4A). We have previously shown that NS5A of genotype 1a (H77C strain), which has an amino acid residue Ile^{121}, was able to interact with FKBP8 (37). To determine the role of Ile^{121} on the binding of NS5A to FKBP8, HA-NS5A(1-125) of the genotype 1b Con1 strain in which Ile was substituted for Val^{121} was coexpressed with Flag-FKBP8 and immunoprecipitated with specific antibodies (Fig. 4B). The HA-NS5A mutant possessing the substitution of Val^{121} to Ile interacted with Flag-FKBP8 at the same level as the wild-type NS5A. Next, to determine the role of Val^{121} or Ile^{121} in the replication of HCV, we generated replicon RNAs in which Val^{121} of NS5A was replaced with either Ala or Ile. In vitro-transcribed RNAs from the pFK-I_{389} hRL/NS3-3′/5.1 carrying the mutation were introduced into the Huh-7 cell line by electroporation. The *Renilla* luciferase activity was measured at 4 and 48 h posttransfection and is represented as the ratio of luciferase activity measured at 48 h posttransfection to that measured at 4 h. The replacement of Val^{121} with Ala severely impaired the RNA replication, whereas substitution of Val^{121} to Ile, as seen in genotype 1a strains, had no apparent effect on the replication (Fig. 4C). These results suggest that Val^{121} and Ile^{121} of NS5A

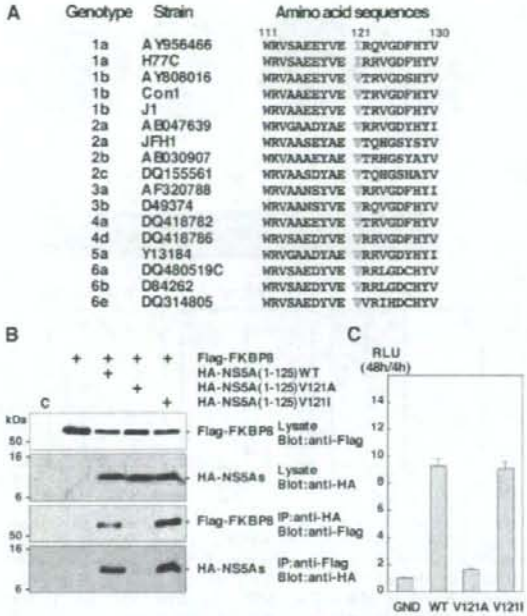

FIG. 4. Effect of the interaction of NS5A with FKBP8 on the transient replication of HCV. (A) Alignment of amino acid sequence of NS5A (111 to 130 amino acids) among different HCV genotypes. Outline letters indicate the amino acid residue at position 121. (B) The substitution mutants of HA-NS5A(1-125) replaced Val^{121} with Ala or Ile were coexpressed with Flag-FKBP8 in 293T cells and immunoprecipitated with anti-HA or anti-Flag antibody. Immunoprecipitates were analyzed by immunoblotting. (C) In vitro-transcribed RNAs from the pFK-I_{389} hRL/NS3-3′/5.1 (wild-type, WT) and those transcribed from the plasmids carrying the lethal mutation in NS5B (GND) or the substitution in Val^{121} to Ala (V121A) or to Ile (V121I) in NS5A were introduced into Huh-7 cells by electroporation. The relative luciferase value was calculated by determining the increase in *Renilla* luciferase activity at 48 h compared to that observed at 4 h after transfection. The relative activity is represented as the ratio of each value of replication efficiency to the corresponding value for GND mutant. The data are representative of three independent experiments.

play crucial roles in the interaction with FKBP8 and the transient replication of HCV replicons. We have previously reported that NS5A interacts with an endogenous FKBP8 in replicon cells harboring the subgenomic viral RNA (37). Therefore, we tried to demonstrate the lack of interaction of FKBP8 with the mutant NS5A substituted Val^{121} to Ala. However, we could not detect a sufficient amount of HCV proteins due to a low level of replication of the subgenomic replicon carrying the mutation in NS5A (Fig. 4C and 5A).

To further confirm the importance of Val^{121} and Ile^{121} in NS5A on the replication of HCV RNA, a colony formation assay was carried out. The replicon RNA carrying a neomycin resistance gene transcribed from pFKI$_{389}$/neo/NS3-3′/5.1 (23) was introduced into Huh-7 cells and cultivated under the pressure of G418. The number of remaining cell colonies was determined at 4 weeks posttransfection. There were more than

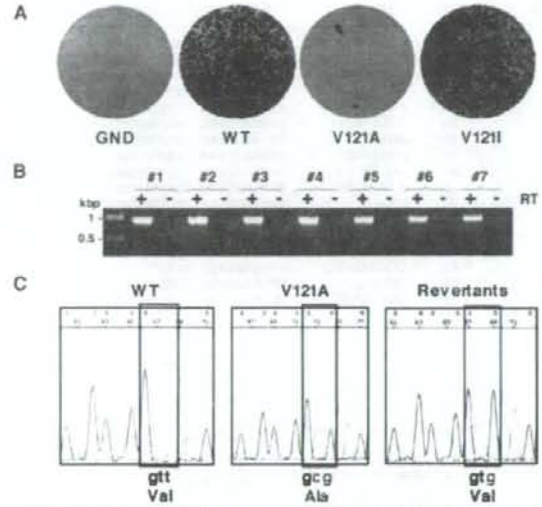

FIG. 5. Effect of the interaction of NS5A with FKBP8 on the colony formation by HCV replicon. (A) The replicon RNAs of the wild type (WT), a replication-deficient mutant (GND), and the substitution in Val^{121} to Ala (V121A) or to Ile (V121I) were transcribed from the plasmids based on $pFKI_{389}$ neo/NS3-3′/5.1, transfected into Huh-7 cells, and selected by G418 for 4 weeks. The remaining cells were fixed in 4% paraformaldehyde and stained with crystal violet. (B) Seven resistant colonies that appeared after transfection with the replicon RNA encoding substitution of Val^{121} to Ala (V121A) in NS5A were expanded, and the total RNAs were purified. The NS5A cDNAs were amplified by PCR with (+) or without (−) reverse transcription. (C) Sequence of NS5A genes derived from the wild type (WT), the V121A mutant, and seven resistant colonies (revertants).

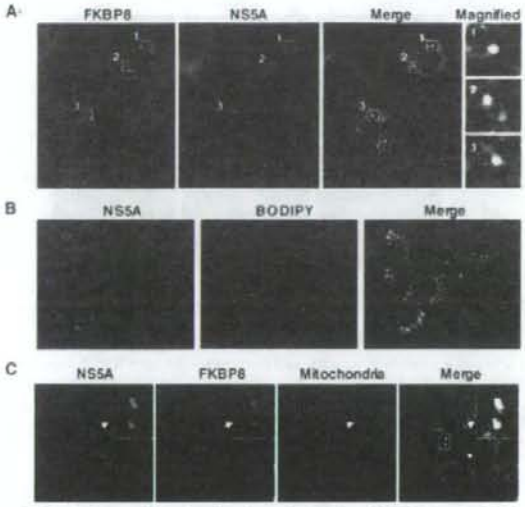

FIG. 6. Intracellular localization of FKBP8 and NS5A in the HCV replicon cells. (A) Huh-7 9-13 cells harboring an HCV subgenomic replicon were fixed with 4% paraformaldehyde in PBS and permeabilized with 0.25% saponin. Endogenous FKBP8 and NS5A were stained with anti-FKBP8 monoclonal antibody (KDM11) and rabbit anti-NS5A polyclonal antibody, followed by staining with AF488-conjugated anti-mouse IgG and AF594-conjugated anti-rabbit IgG antibodies, respectively. Rectangles 1, 2, and 3 were magnified and are shown on the right. (B) NS5A was stained with the rabbit polyclonal antibody to NS5A and AF488 conjugated anti-rabbit IgG. Lipid droplets were specifically stained with Bodipy 558/568 C12. (C) Endogenous NS5A and FKBP8 were stained with stained rabbit anti-NS5A polyclonal antibody and anti-FKBP8 monoclonal antibody (KDM11), followed by staining with AF488-conjugated anti-rabbit IgG and AF546-conjugated anti-mouse IgG, respectively. Mitochondria were stained with Mitotracker Deep-Red. White rectangles indicate the magnified images of the small white inside boxes.

1,000 colonies on the plate of Huh-7 cells into which the parent replicon RNA or an RNA carrying the substitution of Val^{121} of NS5A to Ile was introduced, but only a few colonies appeared on the plate of cells into which RNA carrying the mutation of Val^{121} to Ala was introduced (Fig. 5A). To characterize the colonies emerging on the plate of Huh-7 cells into which the mutant Ala^{121} replicon RNA was introduced, the total RNAs were purified from the seven resistant colonies. The NS5A cDNAs were amplified after reverse transcription but not in the absence of reverse transcription (Fig. 5B), suggesting that the amplified cDNAs were derived from RNA but not from the remaining transfected plasmid DNA. The NS5A genes were subjected to direct sequencing and revealed that the transfected mutant replicon RNA had GCG corresponding to the Ala^{121}, in contrast to the parental replicon, which had GTT corresponding to the Val^{121}. On the other hand, all of the RNAs prepared from the individual resistant colonies had GTG encoding Val (Fig. 5C), indicating that the resistant colonies were not derived from the contamination of the wild-type replicon RNA but emerged by the mutation after replication. These results further support the notion that Val^{121} in NS5A is an indispensable amino acid and plays an important role in the replication of HCV though interaction with FKBP8.

Subcellular localization of FKBP8 and NS5A. Previous reports suggest that FKBP8 is mainly localized on mitochondria (7, 44), whereas NS5A is mainly localized on the endoplasmic reticulum (ER) and Golgi apparatus (2, 6, 16). HCV is reported to replicate in a raft-like intracellular compartment or the folded membranous compartment known as a membranous web in the replicon cells (8, 13, 15). In the present work, intracellular localization of FKBP8 was examined by immunofluorescence staining of the replicon cell line, Huh-7 9-13, which harbored an HCV subgenomic replicon, with the antibodies to NS5A and to FKBP8. Endogenous FKBP8 was mainly found in mitochondria and was partially colocalized with NS5A in a few compartments sharing a dot-like structure (Fig. 6A). Lipid droplets were required for production of infectious HCV (5) and were colocalized with NS5A and core protein (43), although NS5A formed as dot-like structures but was not found in lipid droplets stained with Bodipy 558/568 C12 in the replicon cell line (Fig. 6B). On the other hand, FKBP8 was mainly localized on mitochondria and partially together with NS5A on dot-like structures that were distinct from the mitochondria (Fig. 6C).

To further analyze the subcellular compartments where FKBP8 and NS5A were colocalized, the same fields of Huh-7 9-13 replicon cells were observed with FM and EM by using